



Utrecht
University

TNO



**Storage and disposal potential of the Triassic
Röt Formation in the east of the Netherlands:
Subsurface mapping and facies
interpretation**

R. J. Altenburg

Master thesis

Department of Earth Sciences

Utrecht University

May 2022

Supervisors:

Dr. J.P. Trabucho-Alexandre (UU)

Dr. J. Bartol (COVRA)

Dr. J.H. ten Veen (TNO)

Dr. R. Bouroullec (TNO)

Abstract

Salt formations are used and considered for temporary underground storage and permanent disposal of gas, oil, and (radioactive) waste. To ensure safe storage and disposal, geological information of a salt formation is required. Its thickness, geographic distribution, depth and tectonic history must be understood to predict its likelihood to become affected by future geological processes. Geological information about the salt layer of the Triassic Röt Formation is limited and therefore it is unclear if this Main Röt Evaporite Member is suitable for either temporary storage or permanent disposal.

Distribution, isopach, and depth maps of the Main Röt Evaporite Member in the subsurface below Enschede using 2D and 3D seismic and well log data are presented. These maps have been evaluated in relation to the tectonic evolution of the area to improve the understanding of the geological development of the unit.

The thickness of the Main Röt Evaporite Member in the study area ranges between 10 and 130 m, and the depth of the top is between 300 and 1500 m. This distribution is controlled by Triassic extension and subsequent Cretaceous inversion. The depositional environment of the Main Röt Evaporite Member is a sabkha with salt pans with episodic marine incursions. Due to insufficient thickness, only in a small part of the study area, the member is potentially suitable for storage/disposal. However, based on other storage and disposal concepts, this area is not reliable for storage/disposal of gas, oil, and (radioactive) waste.

Acknowledgements

I would like to thank my supervisor from Utrecht University, João Trabucho. Thank you João, for being my supervisor for the second time, it was an honour. Thank you for your precious time, fun talks, and the detailed feedback you gave on my first versions of this thesis.

With the ending of this master thesis, I also end the internship I have done at COVRA, where my supervisor was Jeroen Bartol. Thank you Jeroen, for our weekly meetings, and discussions, for introducing me to the world of radioactive waste and disposal at COVRA and for the interesting tour through the storage in Zeeland. I also would like to thank the people at COVRA, although I have not been there so often, I enjoyed working there.

This project was also part of an internship at TNO, where my supervisors were Johan ten Veen and Renaud Bouroullec. Thank you, Johan, for your time and knowledge and for answering all the questions I had. Thank you, Renaud, for the comments on my first version and for sharing your knowledge.

Furthermore, I want to express my appreciation to everybody in the geomodelling team at TNO for answering multiple kinds of questions, and of course the coffee talks with Frans.

Lastly, I would like to thank André Slupik from the corehouse in Zeist, for the chats and for carrying all the heavy salt cores with me.

I enjoyed working with all of you and hope to do so again in the future.

Contents

1. Introduction	1
Aim of the study	2
Geological context of the Röt Formation	3
2. Materials and methods	9
Study area	9
Seismic surveys	10
Well data	11
Seismic-to-well tie	12
Seismic interpretation	14
3. Results	15
Seismic to well tie study	15
Depth, thickness, and distribution of the Main Röt Evaporite Member	15
Facies description	19
4. Discussion	28
Tectonic setting and events	28
Palaeogeography and facies distribution	31
Crystalline vs mechanical facies	35
Stratigraphic correlation	37
Assessment of the storage/disposal potential	37
Limitations	39
Recommendations	40
5. Conclusions	42
References	43
Appendix	49

List of figures

Figure 1. Distribution and isopach map of the Röt Formation	4
Figure 2. Stratigraphy of the Triassic	6
Figure 3. Study area for this research	9
Figure 4. Function of sonic and density log	13
Figure 5. Calculations of density log	14
Figure 6. Distribution map	15
Figure 7. Interpreted seismic surveys	16
Figure 8. Interpreted seismic survey	17
Figure 9. Depth map	18
Figure 10. Thickness map	19
Figure 11. Different facies of the Main Röt Evaporite Member	22
Figure 12. Seismic survey with well TWR-480	24
Figure 13. Well section window	26
Figure 14. Structural elements in the Netherlands	29
Figure 15. Depositional setting	34
Figure 16. Assessment for the storage/disposal potential	40

List of tables

Table 1. Seismic surveys used for this study_____	11
Table 2. Key wells with available logs _____	11
Table 3. Facies description and interpretation_____	25

1. Introduction

Salt formations are used and considered for temporary underground storage and permanent disposal of gas, oil, and (radioactive) waste (Cyran, 2020; Kumar et al., 2021). Compared to other rock types, rock salt is special due to its extremely low porosity of less than 1% and a permeability of 10^{-22} to 10^{-19} m², which make the rock virtually impermeable (Geluk et al., 2007). Furthermore, when rock salt is deformed, or when other materials invade it, it can restore its low permeability and sealing properties relatively quickly and it will form a natural barrier around the other material (Spiers et al. 1986; Urai et al., 2008).

In several places around the world, rock salt formations are used to store (liquid) hydrocarbons (e.g., Canada, England, France, Germany, Poland, USA), hydrogen (UK, USA), and compressed air (Germany, UK, USA) (Warren, 2006; Cyran, 2020). In the Netherlands, rock salt is used for underground storage of nitrogen (stikstofopslag Heiligerlee), gas (aardgasbuffer Zuidwending), and gasoil (Neeft et al., in press). Rock salt is also used for waste disposal of, for example, alkali waste of soda production (England, Netherlands, Mexico) and waste from oilfields (Canada, USA) (Warren, 2006; Cyran, 2020).

The properties of rock salt make it potentially suitable to permanently dispose radioactive waste in the subsurface. Although this is a controversial subject, due to safety reasons, this already happens in the United States in the Waste Isolation Pilot Plant (WIPP) in the Salado bedded salt formation

(Hansen et al., 2016; Neeft et al., in press; Warren, 2006). In Germany, the Morsleben repository for radioactive waste was constructed in Zechstein strata (Behlau & Mingerzahn, 2001) and operations and research have been undertaken at the Asse and Morsleben domes (Hansen et al., 2016). Salt formations are promising potential candidates for the disposal of radioactive waste in the future (Hunsche & Hampel, 1999).

In the Netherlands, the salt of the Triassic Röt Formation is considered to be one of the host rocks for deep geological disposal of radioactive waste by COVRA, the central organization for radioactive waste in the Netherlands (Verhoef et al., 2017). To assess the storage and disposal potential of this formation, detailed information (on the geological development) is required. This is necessary because a repository will be there for centuries and geological processes that will happen in the future have to be taken into account. Which processes the formation was involved in the past will tell us something about how stable a formation will be in the future.

Aim of the study

This study aimed to gather geological information about the Main Röt Evaporite Member of the Triassic Röt Formation relevant for its utilization as storage or deposit of waste. The main parameters of interest were the geographic distribution of the unit, its thickness, depth, and the internal heterogeneity of its facies. This thesis addresses the stratigraphical and tectonic development of the Triassic Main Röt Evaporite Member to enable COVRA to understand whether this layer is potentially suitable for deep

geological disposal. This is done in a study area in the East of the Netherlands.

To achieve this aim the following objectives need to be met:

1. Present a distribution, isopach, and base map of the Main Röt Evaporite Member
2. Present facies description – characterize the stratigraphic architecture of the unit.

Geological context of the Röt Formation

The tectonics and stratigraphy of the Triassic in the Netherlands have been particularly well studied (e.g., Geluk & Röhling, 1997; Geluk, 2005; Geluk, 2007; McKie & Kilhams, in press). However, the Main Röt Evaporite Member of the Röt Formation in the Netherlands has never been studied in detail.

The Röt Formation is composed of interbedded evaporites, claystones, siltstones, and sandstone units. In the Netherlands, the formation was preserved in the Dutch Central Graben, West Netherlands Basin, around the Groningen High, and in the Central Netherlands Basin (Fig. 1).

There are four members in the Röt Formation, two evaporitic layers: the Main Röt Evaporite Member and the Upper Röt Evaporite Member,

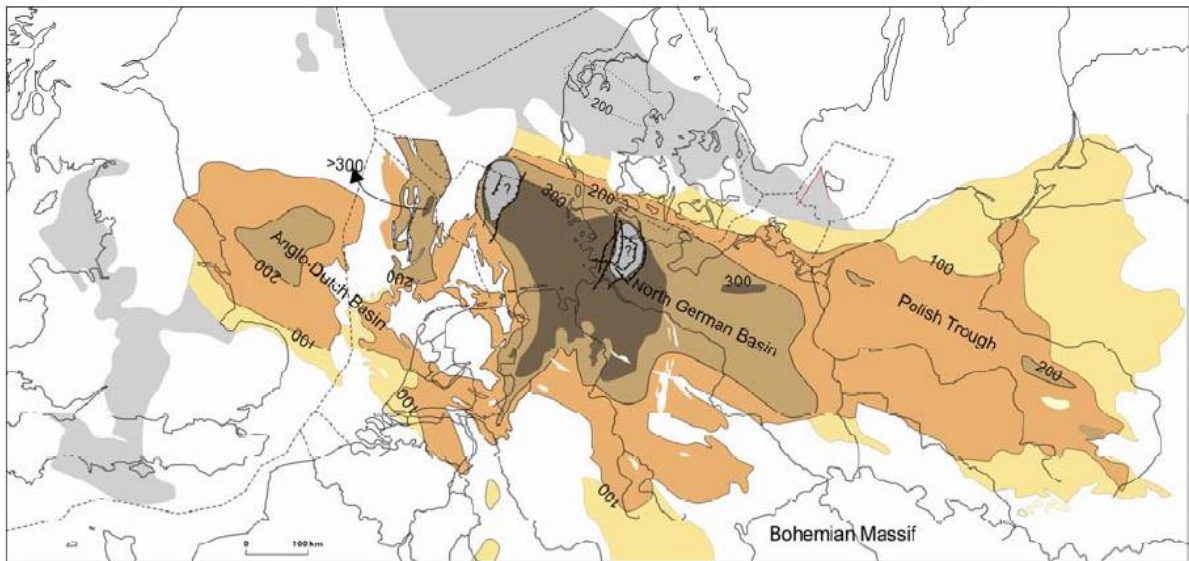


Figure 1. Present-day distribution and isopach map of the Röt Formation. Across North and central Europe the thickness of this Formation varies from 0 to 300 m. In the areas with grey shading, the thickness is uncertain. (After Wolburg (1969), Bertelsen (1980), Cameron et al. (1992), Dadlez et al. (1998), Geluk (1999), Baldschuhn et al. (2001) Goldsmith et al. (2003) and Geluk (2005).

separated by a claystone member: the Intermediate Röt Claystone Member and on top, there is the Upper Röt Claystone Member. This research focused on the Main Röt Evaporite Member since it is more widespread and thicker than the Upper Röt Evaporite Member.

The thickness of the Main Röt Evaporitic Member varies between 30 m to over 150 m in the Broad Fourteens and Central Netherlands Basins and is up to 300 m in the Dutch Central Graben (van Adrichem Boogaert & Kouwe, 1994; Geluk, 2005; TNO-GSN, 2021). Within the Main Röt Evaporite Member, four different salt layers have been distinguished by the mining company Akzo Nobel (now Nubian), salt A to D (Harsveldt 1980; van Lange 1994; Kovalevych et al. 2002). Whereas salt layer A is the thickest (10-50 m), B ranges from 1 to 7 m, salt C is around 20 m thick and D, which is a few meters thick, is locally distributed as lenses in

paleotopographic lows. Between these salt layers, 1-2 m thick layers of claystone, anhydrite and polyhalite are present. (Harsveldt 1980; NITG, 1988; van Lange 1994; Urai & Schléder, 2005). In general, the member grades locally into sandstones towards the south, the Röt Fringe Sandstone (Geluk, 2005).

The Triassic in the Netherlands has been divided into the Lower Germanic Trias Group and the Upper Germanic Trias Group, separated by the Hardegsen Unconformity (Van Adrichem Boogaert & Kouwe, 1994) (Fig. 2). The Lower Germanic Trias Group (latest Permian-Olenekian), consisting of the Lower- and Main Bundsandstein Formations, mainly fine-grained clastic deposits with sandstone and oolite intercalations (Geluk, 2007). The Röt Formation, together with the Solling, the Muschelkalk, and the Keuper Formations, forms the Upper Germanic Trias Group (Olenekian-Norian) in the Netherlands, an alternation of fine-grained clastics, carbonates and evaporites.

The base of the Upper Germanic Trias Group, the Hardegsen Unconformity, represents the first major extensional phase in the Triassic, known as the Hardegsen phase (Ziegler, 1990; Geluk & Röhling, 1997, 1999; Geluk, 2005). The Hardegsen extensional phase formed an E-W trending basin in northwestern Europe, the southern Permian basin, where fluvial and playa

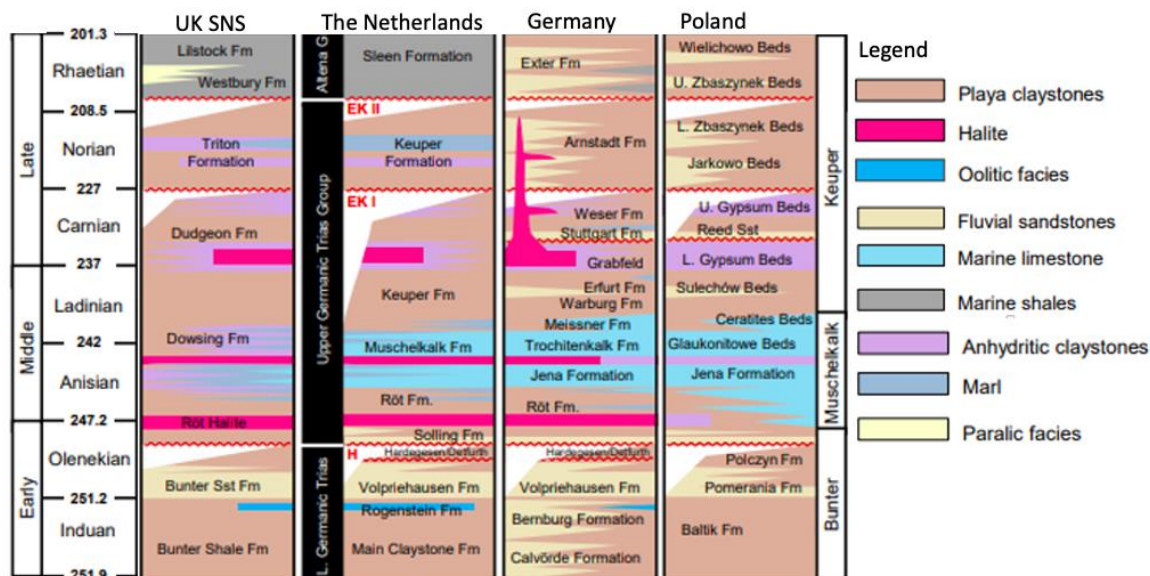


Figure 2. *The stratigraphy and dominant facies of the Triassic in the Southern Permian Basin area. EK I and II present the Kimmerian unconformities, UK SNS = United Kingdom Southern North Sea. The halite facies from the Röt Formation can be found in Germany, the Netherlands and in the UK. After Mckie & Kilhams (in press).*

depositional facies developed: the Solling Formation - a sandstone with overlying claystone (Geluk, 2005; TNO-GDN, 2022).

The Röt Formation marks the first major access of the Tethys Ocean into this basin (Kovalevytch, 2002; Geluk, 2005). The Tethys ocean came into the basin via the Silesian-Moravian Gateway and East Carpathian gates in Southern Poland (Ziegler, 1990; Geluk, 2005; 2007). From time to time there was limited access to open marine waters in the Western Southern Permian Basin because the Szczecin-Wolsztyn Swell in Poland caused a restricted connection. This caused an alternation of evaporite facies – the Main Röt Evaporite Member and the Upper Evaporite Member – alternated with argillaceous members– e.g. the Röt claystone Member- which created mudflats where marine fauna lived (Geluk, 2005; Kovalevytch et al., 2002; Diedrich, 2009). During the deposition of the Röt Formation, the

Netherlands was part of an extensive sabkha with dry climatic conditions (Geluk, 2005). During the Late Anisian, subsidence caused major access by Tethyan marine waters in the basin where transgressive depositional facies developed and flooded the entire Southern Permian B area which formed the Muschelkalk Formation (Geluk, 2005; 2007; Bachmann et al., 2010).

The Röt Formation covers a large area of the UK, Dutch, Danish and German parts of the Southern Permian Basin, and can be identified based on their palynological assemblages, however, other countries have different members and names (Kovalevytch, 2002; Geluk, 2007). Overall it is presumed that the Röt Formation covers an evaporite facies that is deposited in a large brackish-water lagoon, with deposits of fine-grained predominantly red clastics from which the name 'Röt' is derived in Germany (Bachmann et al., 2010).

In Germany, the Triassic has been split up into three groups, the continental Buntsandstein Formation, the marine Muschelkalk Formation and the continental, brackish and hypersaline Keuper Formation, each of which is divided into three subgroups (Bachmann et al., 1999). Here, the Röt Formation is part of the Upper Buntsandstein group (Bachmann et al., 2010).

Where the connection with the Tethys ocean was established, in Southern Poland, through the Silesian/Moravian and East Carpathian gates, different facies developed. In the Röt Formation of Southern Poland there are

calcareous members, 'Rötdolomit' and 'Rötkalk', suggesting a more open marine environment (Trammer, 1972; Kozur, 1975).

As the marine conditions extended westwards to the central German area there was marine fauna in the Röt Formation (bivalves, cephalopods and reptiles) (Bachmann et al., 2010).

Almost all the Members of the Dutch Röt Formation and the Muschelkalk Formation can be found in the United Kingdom and Southern North Sea area due to their similar lithology, and therefore depositional setting (Southworth, 1987). The Main Röt Evaporite Member is here called the Main Röt Halite Member and is part of the Dowsing Formation (Southworth, 1987).

The preservation of the Triassic strata highly depends on the rate of subsidence of the extensional phases in the Triassic and further on in the Jurassic. The Late Cretaceous was a period of inversion and thus erosion. During this time almost all the Triassic strata, except for the basins that were formed due to extensional phases were eroded. The basin-margin successions are equally poorly preserved for the same reason (McKie & Kilhams, in press).

2. Materials and methods

Study area

The study area covers approximately 6400 km² in the east of the Netherlands (Fig. 3). This area was selected because, although the Main Röt Evaporite Member is deposited largely offshore in the Netherlands, a repository for waste has to be onshore. This was agreed on in the ‘London Convention’ – a global convention to protect the marine environment from human activities (International Maritime Organization, 1972). Furthermore, a repository has to be built within ≈ 100 years thus existing building techniques need to be used to build the repository (Verhoef, 2017). For this reason, the depth target of a potential host formation must lie between 500 – 1500 m depth as storage and deposit caverns can be constructed at this depth with existing techniques (Donadei & Schneider, 2016). In the north of

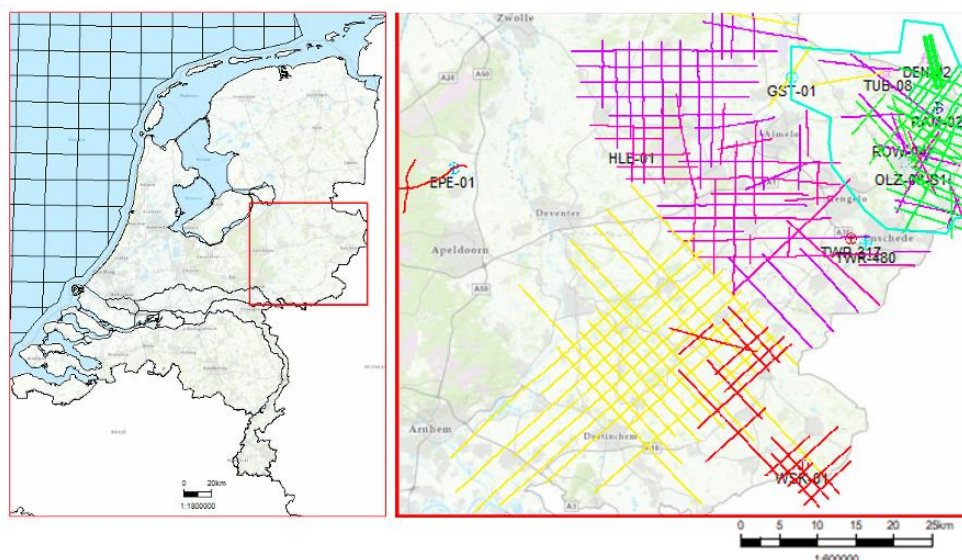


Figure 3. The study area for this research in the east of the Netherlands with seismic surveys and key wells. A square with coordinates of the top left corner: 52°31'33.2"N, 5°49'36.5"E. Colours of the seismic surveys correspond to table 1, Table 2 is a list of the key wells shown on this map.

the Netherlands, the Main Röt Evaporite Member approximately lies between 2 and 3 km depth, while in the east of the Netherlands, the Röt Formation is only 200 to 500 m deep (NITG, 1998).

Besides building with existing techniques, the depth of the host formation should be sufficient to protect the facility from the effects of geomorphological processes such as erosion and glaciation during ice ages (Verhoef, 2017). In the past, geological formations have been affected by erosion of melting ice sheets and features referred to as tunnel valleys formed (Verweij, 2016). The probability of major erosion by future glaciation over a period of 1 million years in the Dutch territory is moderate in the northern onshore and southern offshore and negligible in the central and southern Dutch onshore (ten Veen, 2015).

Lastly, this area is favourable due to plenty of wells with log information on the Main Röt Evaporite Member and the many seismic surveys in the area which will be used. For these reasons, the area in the east of the Netherlands was chosen.

Seismic surveys

To establish distribution, top, base and isopach maps of the Main Röt Evaporite member in the study area, seven 2D surveys and one 3D seismic survey, with a total of 150 seismic lines, were studied (Table 1, appendix).

The top and the base of the Main Röt Evaporite Member have been interpreted in Petrel (Schlumberger) with a University of Utrecht donated

license for student usage. Subsequent horizons are interpreted with the help of existing data from the TNO database. The Society of Exploration Geoscientists (SEG) convention was used in all seismic data: an increase in acoustic impedance results in a negative response and a blue seismic loop, and a decrease in acoustic impedance results in a positive response and a red seismic loop. The average vertical resolution of the seismic data on the Röt level is c. 20 m. This is the minimum thickness that a unit needs to visualize the base and the top of this unit separately.

Well data

In the study area, 627 boreholes containing lithostratigraphic information on the Main Röt Evaporite Member are available. However, complete well log information (density, sonic, gamma-ray) is not available for every well. Therefore, 12 key wells were chosen based on log data, position, and thickness (Table 2, Fig. 3).

Table 1. *Seismic surveys used for this study, colours respond to figure 3.*

	Name	Year of aquisition	Company	Type
1	L2NAM1970	1970	NAM	2D
2	L2NAM1971	1971	NAM	2D
3	L2NAM1972	1972	NAM	2D
4	L2NAM1973	1973	NAM	2D
5	L2NAM1975	1975	NAM	2D
6	L2NAM1982	1982	NAM	2D
7	L2PET1983D	1983	Delft Geophysical	2D
8	L3NAM1993A	1993	NAM	3D

Table 2. *Key wells with the available logs and closest seismic survey. GR = Gamma-ray log, DT = Sonic log, Rho = density log.*

	Well identifier	GR	DT	Rho	Seismic survey
1	DEN-02	x	x		726008
2	EPE-01	x	x	x	1463516
3	GST-01	x	x	partly	726008
4	HLE-01	x	x	partly	706028
5	OLZ-08-S1	x	x		732206
6	RAM-02	x	x	partly	823121
7	ROW-04				716066
8	TUB-08	x	x	partly	726008
9	TUM-01	x	x	partly	726006
10	TWR-317	x			823124
11	TWR-480	x			716032
12	WSK-01	partly	x		751064

The top and the base of the Main Röt Evaporite Member are based on the subdivision of the Röt Formation by Van Adrichem Boogaert & Kouwe (1994). However, the exact top and the base of this member have never been determined. For this reason, the core of TWR-480 was studied in detail, to characterize the unit in terms of facies and their heterogeneity.

Seismic-to-well tie

Well-logs are recorded in-depth and seismic reflectors are recorded in time. For this reason, synthetics were made of the 12 key wells (Table 2) to link the depth to the specific seismic reflector (top Main Röt Evaporite Member) in time (s).

Synthetics were made by using the seismic-well-tie process in Petrel. For the seismic to well-tie process density, sonic, and checkshot data are required. For the 12 key wells sonic and checkshot data are available, density log only for one (EPE-01). For the 11 wells without a density log an alternative method to calculate the density log was necessary. This was done in 2 ways:

1) using Gardner's equation. Gardner's equation describes the relationship between the density and sonic logs and is used when the density log is not, or only partly, available (Gardner et al., 1974) (Eq. 1).

$$\rho = \alpha V_p^\beta$$

Equation 1. *Gardner's equation. Where ρ is bulk density given in g/cm^3 , V_p is P-wave velocity given in ft/s, and α and β are empirically derived constants that depend on the geology. For this research there was taken: $\alpha = 309.45$ and $\beta = 0.25$. After Gardner and others (1974).*

2) using the relation of the density log and the sonic log of the EPE-01 well (Fig. 4). It is possible to calculate the density from the sonic because of the relation between the sonic (travel time) and the density of a formation. This relation was used to calculate the density log of the other wells with their sonic log.

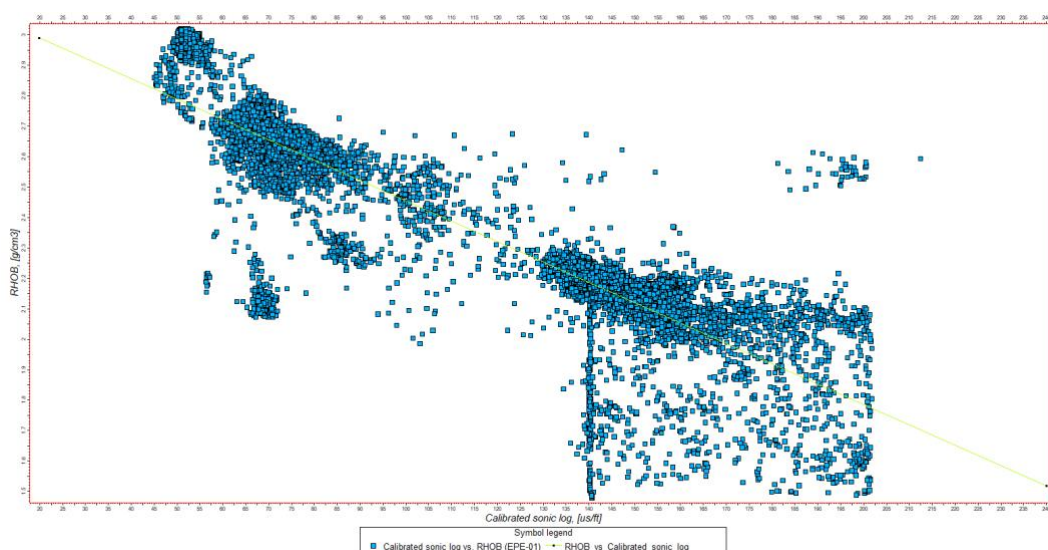


Figure 4. The sonic log (Calibrated sonic log) as function of the density log (RHOB) of EPE-01 well. The function that describes this is: $Y = -0.007x + 3.12$.

Both methods to calculate the density log were carried out and compared.

The result of this was so similar that there was concluded that both methods are good and I decided to calculate the other density logs via method 1, Gardner's equation (Fig. 5). After the density was calculated for the key wells the seismic to well tie process was done and synthetics were made whereafter the two-way travel time (TWT) and the depth of the top and the base of the unit were extracted from the seismic.

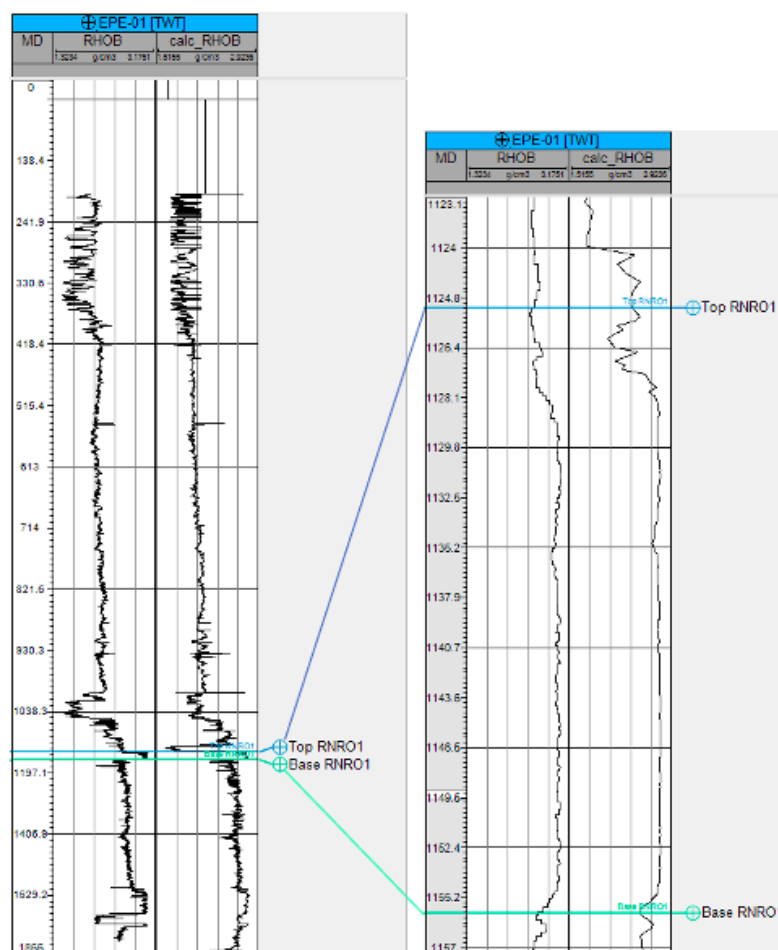


Figure 5. The density log of well EPE-01 was the only density log available in the study area. RHOB shows the actual density log and calc_RHOB the density log calculated with the relation of the density and the sonic log: $Y = -0.007x + 3.12$. The results are similar, where RHOB shows peaks, the calc_RHOB gives this as well.

Seismic interpretation

By using the synthetics of the 12 key wells, seismic interpretation of the top and the base of the Main Röt Evaporite Member was carried out on the seismic survey closest to the well (Table 2, Fig. 3). From these 12 interpreted surveys the interpretation was extrapolated towards other seismic surveys. When all seismic surveys were evaluated, a distribution, an isopach, and base maps were produced. The seismic interpretation was done by the 2D seeded autotrack tool in combination with the 3D seeded autotrack tool in Petrel.

3. Results

Seismic to well tie study

The seismic to well tie process showed that the top of the Main Rot Evaporite Member is a decrease in seismic impedance and therefore is a trough (blue reflector) and the base of the member is an increase in seismic impedance and is, therefore, a peak (red reflector).

Depth, thickness, and distribution of the Main Röt Evaporite Member

Distribution

The distribution of the Main Röt Evaporite Member in the study area is mainly defined by angular unconformities in the south and north of the unit (Figs 6, 7). At the North, South and Western boundary, the North Sea Group

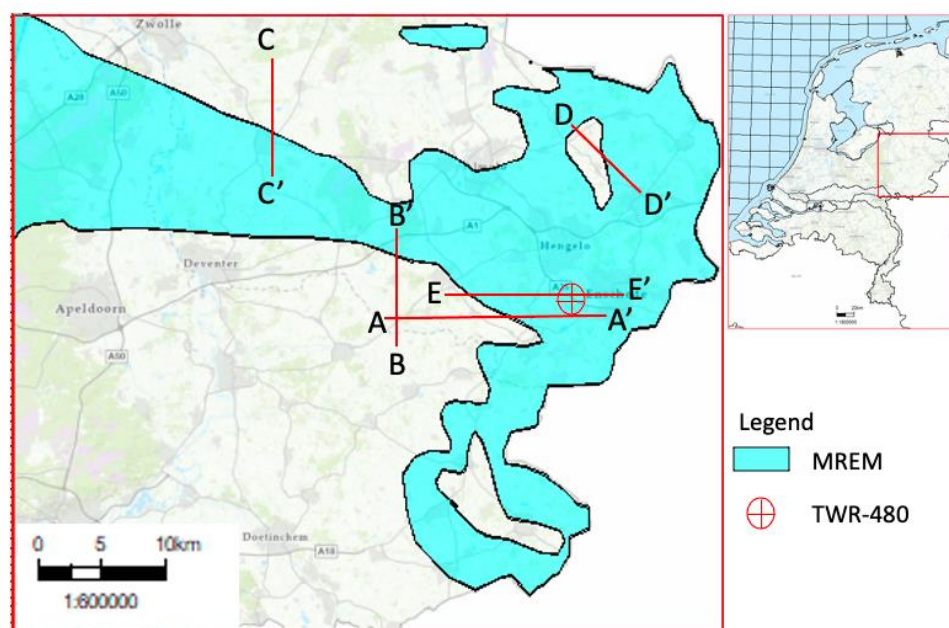


Figure 6. Distribution of the Main Röt Evaporite Member throughout the study area. MREM = Main Röt Evaporite Member.

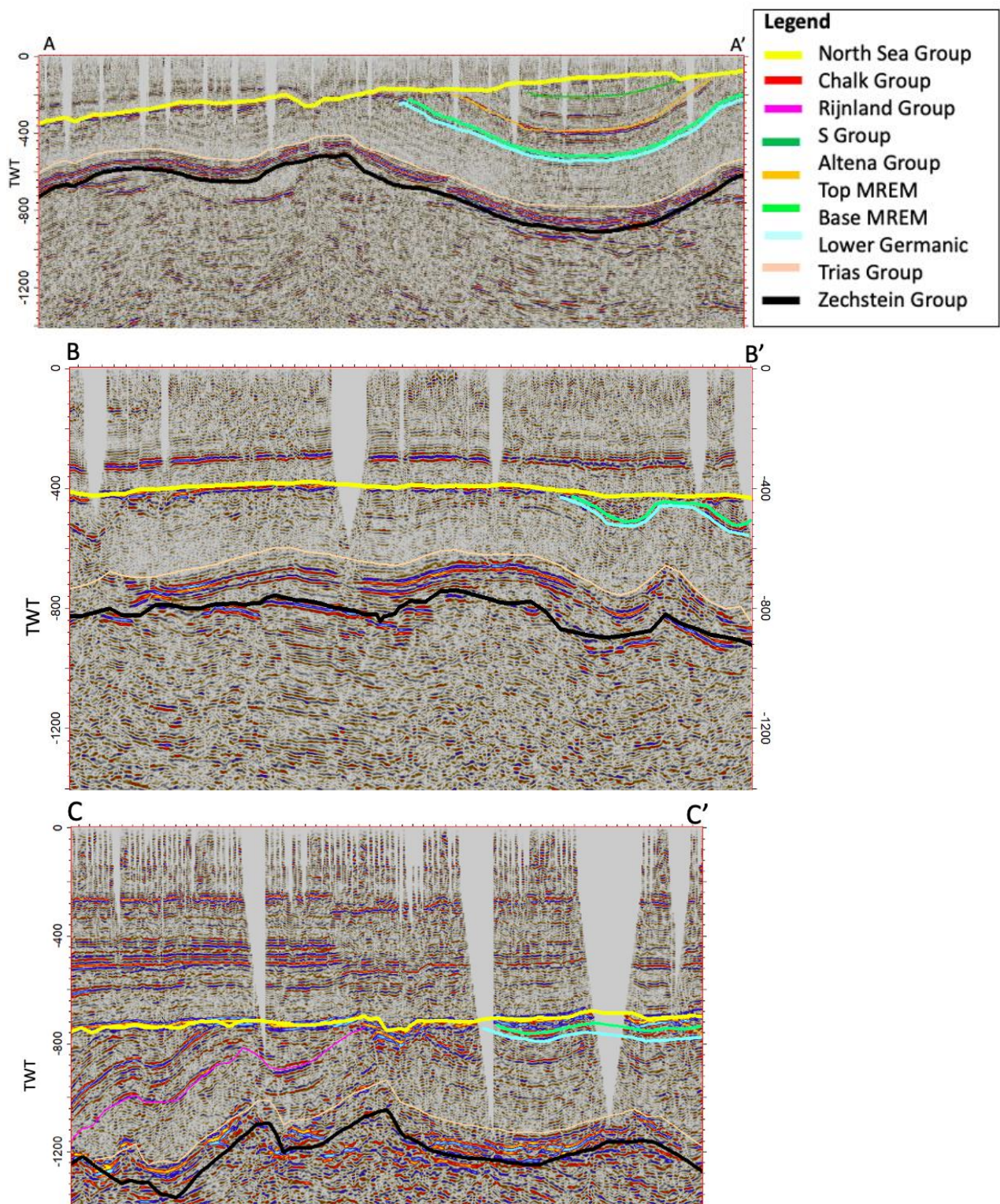


Figure 7. Seismic survey 706036 (top), seismic survey 706025 (middle) and seismic survey 716025 (bottom) with interpreted horizons. An angular unconformity is visible here: the North Sea Group lies on top of the Main Röt Evaporite Member. Furthermore, synclines and anticlines are visible which suggests tectonic movement between the deposition of the S Group and the North Sea Group.

lies directly on top of Mesozoic strata, which represents a hiatus of ≈ 180

million years. Within the deposited unit in the study area, also

unconformities are observed, probably caused by folding (Fig. 8).

Throughout the whole study area, synclines and anticlines are visible, the

Main Röt Evaporite Member, together with the underlying strata has been

folded between deposition of the S Group and the North Sea Group with an

amplitude of ≈ 400 m (Fig. 7).

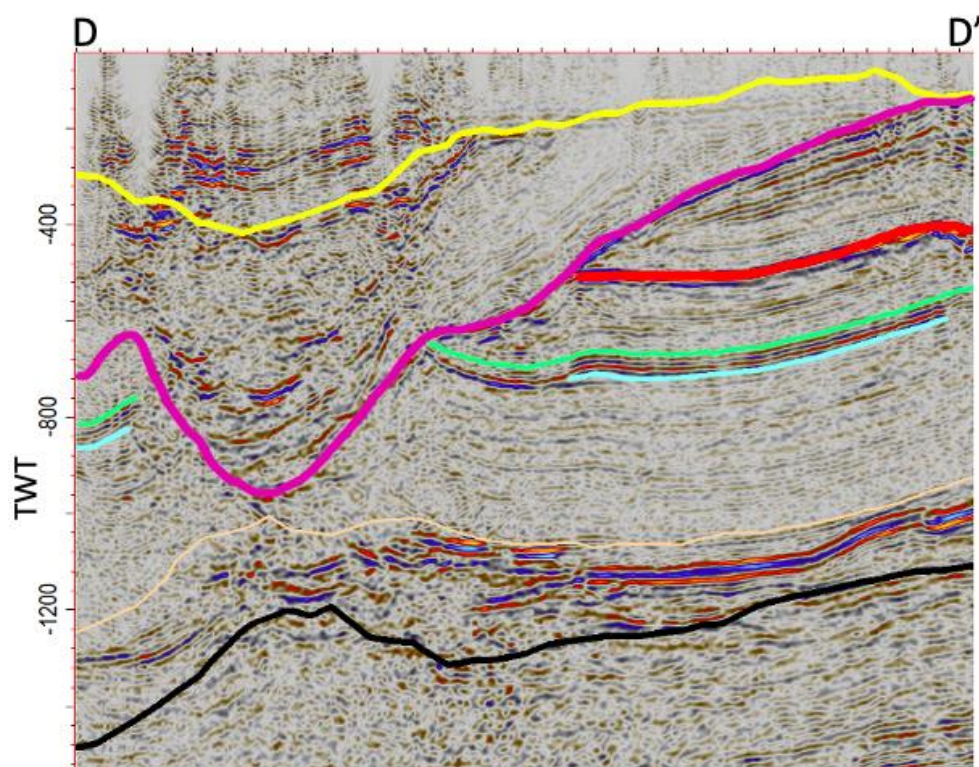


Figure 8. Seismic survey 732208 with interpreted horizons. This shows an area without Main Röt Evaporite Member in the northeast part of the study area. Erosion between deposition of the Röt and the Rijnland Group caused an unconformity causing Rijnland Group on top of the Main Röt Evaporite Member while the Lower Germanic Trias and Zechstein groups show an antiform. For legend see figure 7.

Depth

The depth of the top of the Main Röt Evaporite Member varies greatly

throughout the study area from ≈ 150 to ≈ 1450 m (Fig. 9). The member is

deepest in the north, near Tubbergen, and towards the west, near Zwolle,

where it lies at >1000 m depth. The member is shallowest near the eastern border, with Germany, in the southeast of the study area, where it lies at about 200 m depth.

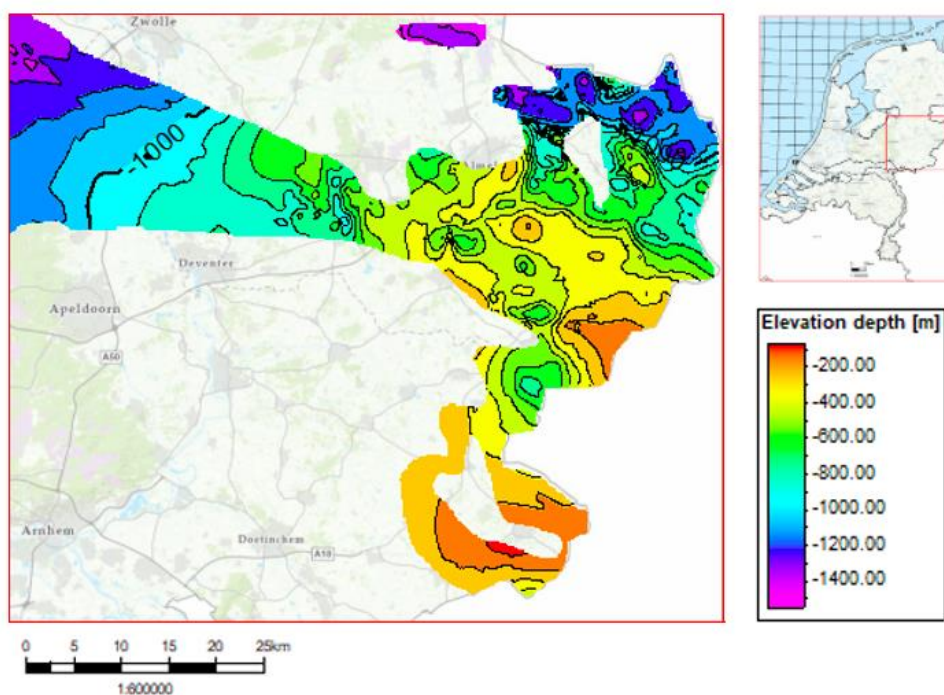


Figure 9. Depth map of the Main Röt Evaporite Member in the study area. The depth is the depth of the top of the member. It shows significant differences in the depth in the study area, in the north, the depths up to 1400 meters are reached while in the south it becomes shallower than 200 meters.

Thickness

The member is thickest in the central part of the study area, around Enschede where it is nearly 120 m thick, and in the north, around Tubbergen, where it also lies relatively deep (Fig. 7). A relation between the thickness and the depth in the north of the study area is possible. In much of the study area the member is relatively thin (< 50 m).

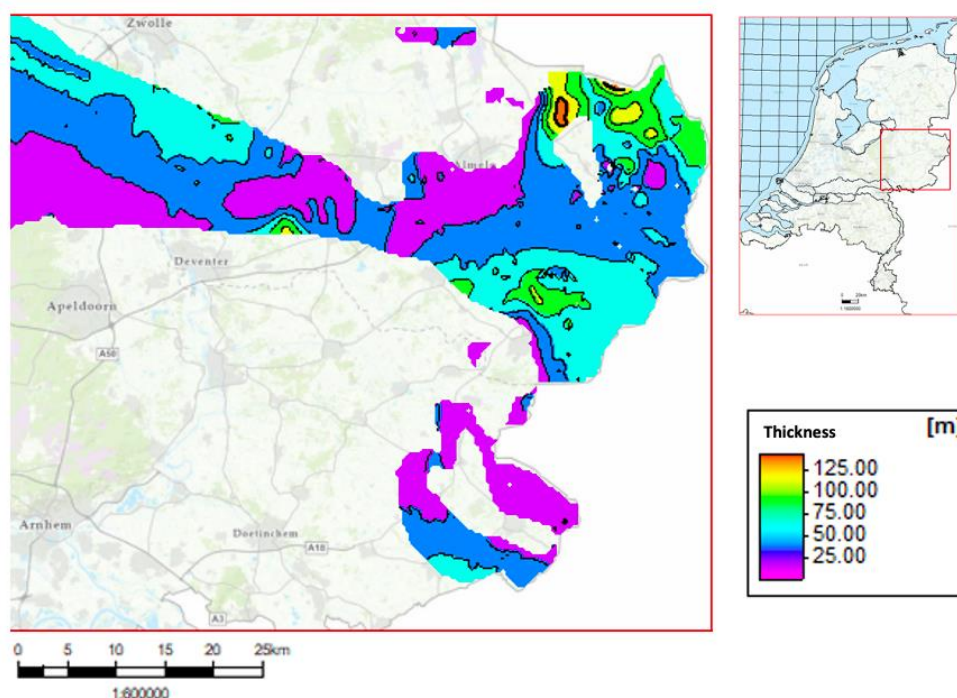


Figure 10. Thickness map of the Main Röt Evaporite Member in the study area. The member is the thickest in the north and in the central part of the study area where it reaches above 100 m. In most of the study area the thickness is relatively thin, < 50 m.

Facies description

The thickness of the Main Röt Evaporite Member in the studied well (TWR-480) is ≈ 83 m. Although its name has ‘evaporite’ in it, this member consists of far more than crystalline evaporites. Primary microcrystalline halite and coarsely crystalline -deformation-related- halite are alternated in combination with clay and sedimentary structures. The different facies present in this well are a product of depositional, diagenetic and deformation processes over time. The studied section can be divided into 10 distinct depositional facies based on lithology and sedimentary structures (Fig. 11). Mineralogy is based on a lithological study of cutting samples of this well (Geowulff Laboratories).

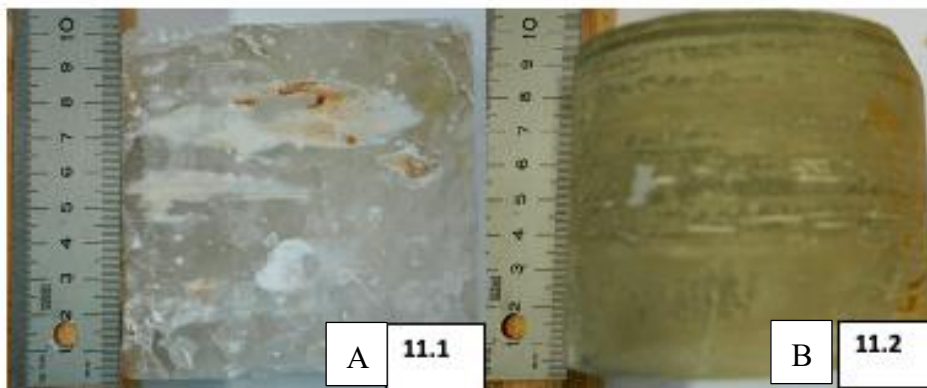


Figure 11 continues on page 21 and 22.



E 11.5



11.5 detail



F 11.6



11.6 detail

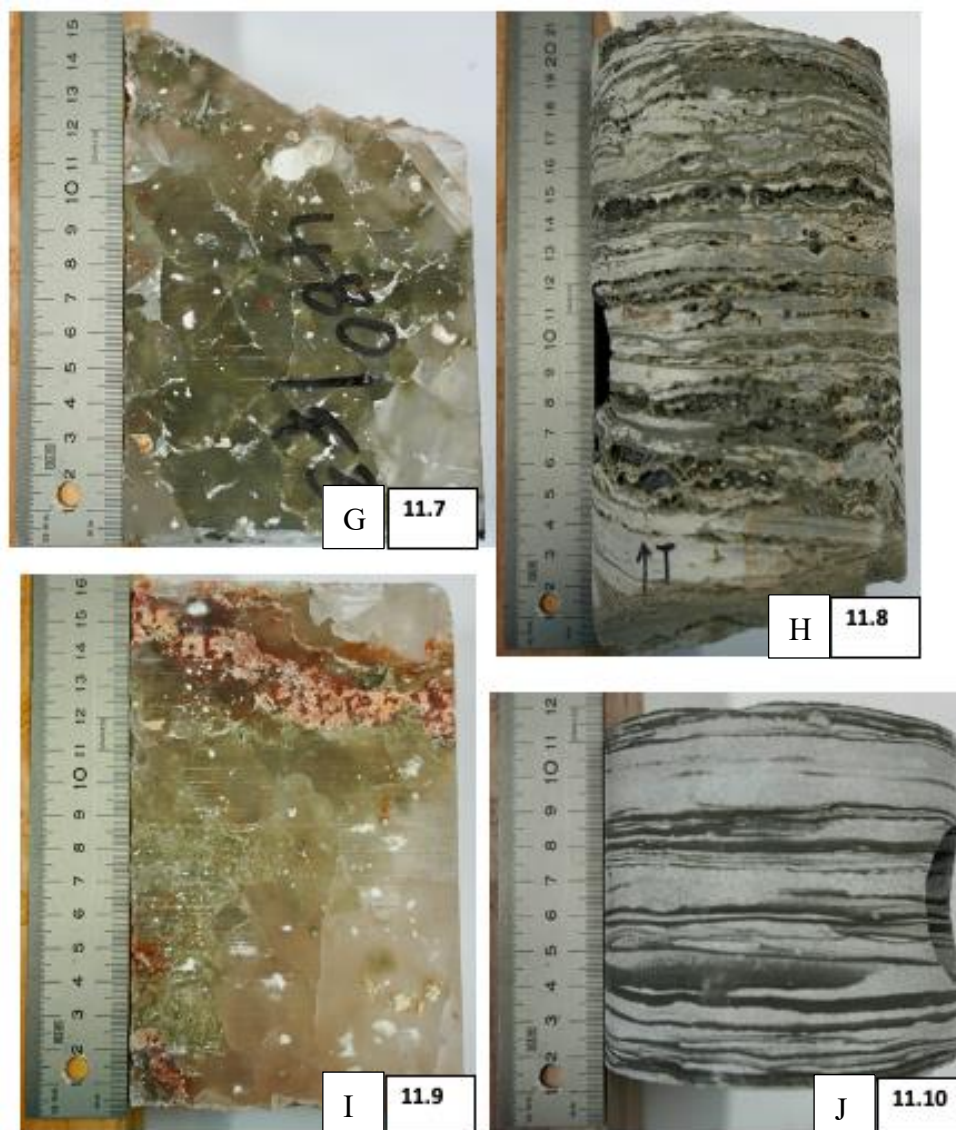


Figure 11. Photographs of the different facies of the Main Röt Evaporite Member of well TWR-480. The top is always in upward direction. Note that facies C has two photographs and facies E and F have detail photographs, showing the brecciated halite and halite patches. The Main Röt Evaporite Member of well TWR-480 shows an alternation of microcrystalline facies (A, D, G, I) and coarsely crystalline facies (C, E, F, H) a dolomite facies (B) and facies with sedimentary structures (G, H, J). Table 3 shows the description and interpretation.

At the base of the studied section, there is the transition of the Solling Formation towards the basal facies A. The Solling Formation has been described as grey sandstone and red claystone in a lacustrine environment (*TNO-GDN (2022)*). There is a sharp transition towards the first facies of the Main Röt Evaporite Member, facies A.

Primary microcrystalline halite facies

There are four clear crystalline halite facies in this member varying in colour from clear to white to red (facies A, D, G, and I) (Fig. 11.1, 11.4, 11.7, 11.9). These microcrystalline facies all have (<5%) inclusions of argillaceous material of red to brown claystone. The transition of these microcrystalline halite facies to other facies is at every transition sharp.

Coarsely crystalline deformation-related halite facies

Several facies in this member include coarsely crystalline halite facies (facies C, E, F, and H) (Fig. 11.3, 11.5, 11.6, 11.8). Coarsely crystalline halite is observed in inclusions in clay (facies F) (Fig. 11.6), alternated with anhydrite and laminated clay (facies C) (Fig. 11.3), in the form of fault breccia surrounded by clay and anhydrite (Fig 11.5) or in nodules in a matrix of clay with sedimentary structures (facies H) (Fig. 11.8). These coarsely crystalline facies are more porous than the microcrystalline halite facies in this member.

Sedimentary structures

There are several sedimentary structures observed in the studied section: chicken-wire structures (facies D) (Fig. 11.4), load-cast structures (facies H) (Fig. 11.8), cross-bedding (facies C) (Fig. 11.3) and current ripples (facies J) (Fig. 11.10).

A summary of facies description is shown in Table 3 and Figure 12 shows the corresponding seismic survey.

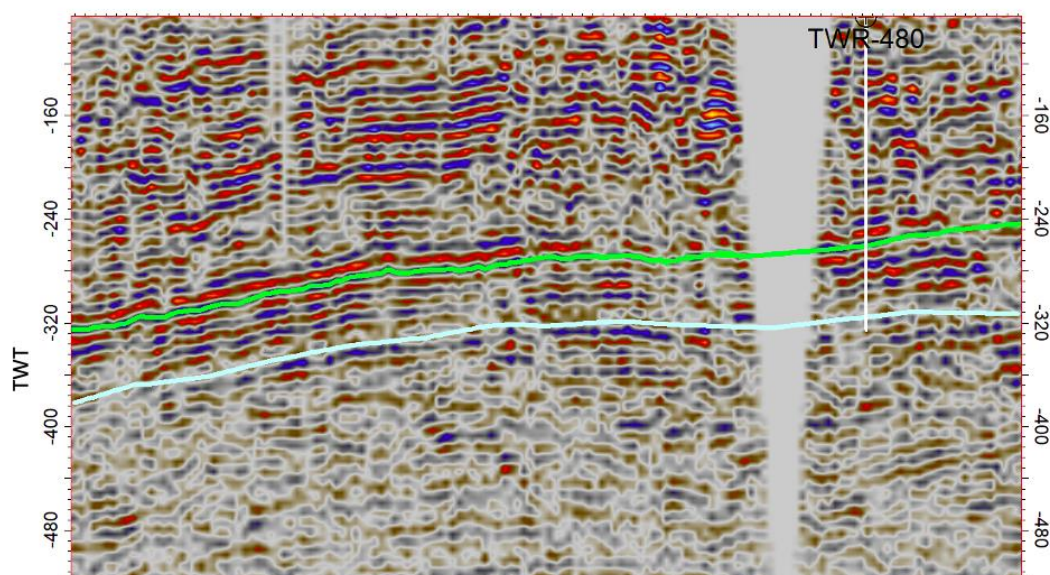


Figure 12. Seismic survey 716032, which includes well TWR-480 which was studied. On the survey the different facies can be distinguished by the variation of amplitude within the Main Röt Evaporite Member. For legend, see figure 7.

Table 3. *Facies description and interpretation of the Main Röt Evaporite Member of well TWR-480. Microcrystalline and coarsely crystalline facies are alternated and different sedimentary structures are present. The yellow marked facies represent the four clear crystalline halite facies. For the description of the facies interpretation see the discussion section.*

J – Fig. 11.10	11.5 m	Grey clastic mudstone with 1mm to 1.5 cm thick white microcrystalline halite layers.	Lenses, wave ripples, current ripples within the halite layers	Sabhka
I – Fig. 11.9	3 m	Red microcrystalline halite with (<5%) argillaceous grey subangular claystone inclusions of granule size, poorly sorted.		Salt pan
H – Fig. 11.8	4.5 m	Light grey claystone with ±2mm dark grey microcrystalline halite layers alternated with layers of 1 - 2 cm interlocking coarsely crystalline halite crystals in a matrix of clay.	Load cast structures	Salt pan
G – Fig. 11.7	18 m	Clear microcrystalline halite with (<5%) argillaceous red subangular claystone inclusions of granule size, poorly sorted.		Salt pan
F – Fig. 11.6	2 m	Red coarsely crystalline halite with 0.5 cm thick anhydrite layers and coarsely crystalline halite in patches surrounded by grey clay,	Fault breccia	Redeposited halite
E – Fig. 11.5	2 m	Red claystone with coarsely crystalline grey halite patches which are very poorly sorted throughout the claystone.		Redeposited halite in clay from fault blocks
D – Fig. 11.4	3 m	Light grey microcrystalline halite with (5%) anhydrite surrounding it in chickenwire structures.	Chicken wire structures	Sabhka
C – Fig. 11.3	2 m	Alternation of white coarsely crystalline halite, laminated grey claystone, dark grey halite with efflorescent halite alternated with chevron halite in a matrix of anhydrite and clay.	In the grey claystone, there is cross-bedding with coarsely crystalline halite	Sabhka
B – Fig. 11.2	1 m	Grey laminated anhydritic dolomite. The laminae have a thickness of 1 - 2 mm.		Hypersaline lagoon
A – Fig. 11.1	36 m	Clear microcrystalline halite with (<5%) argillaceous red subrounded claystone inclusions of granule size, poorly sorted.		Salt pan

The facies description of well TWR-480 shows representative facies for the rest of the unit. Where it has approximately the same thickness, the same responses in the gamma log are observed. However, the unit is in most of the study area a lot thinner and the depth alternates significant throughout the research area, therefore the exact present facies in the thinner units is hard to determine (Fig. 13).

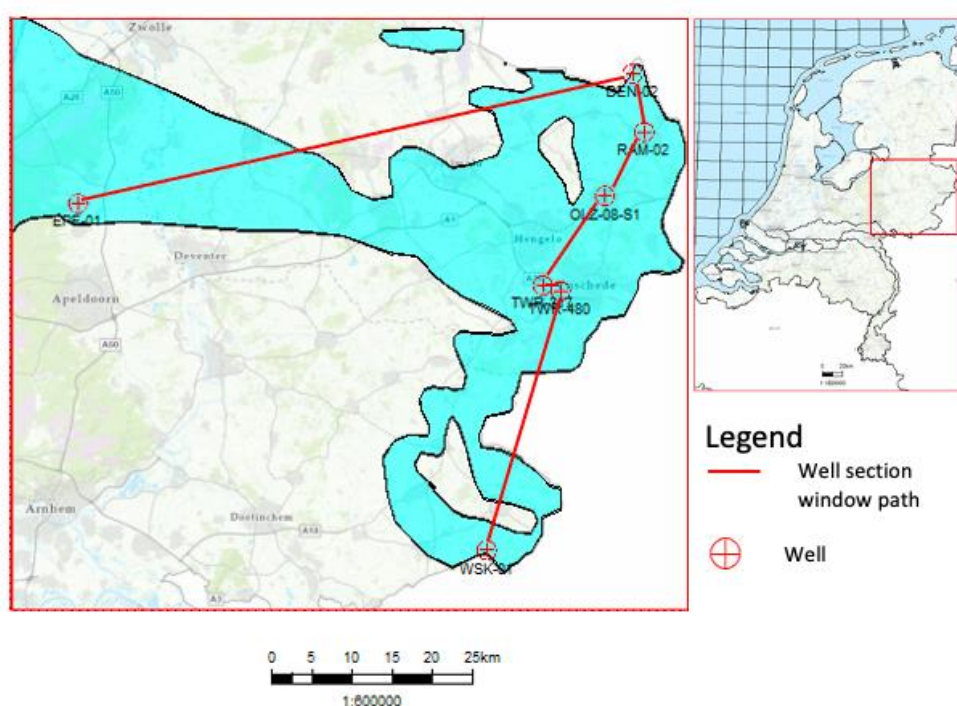
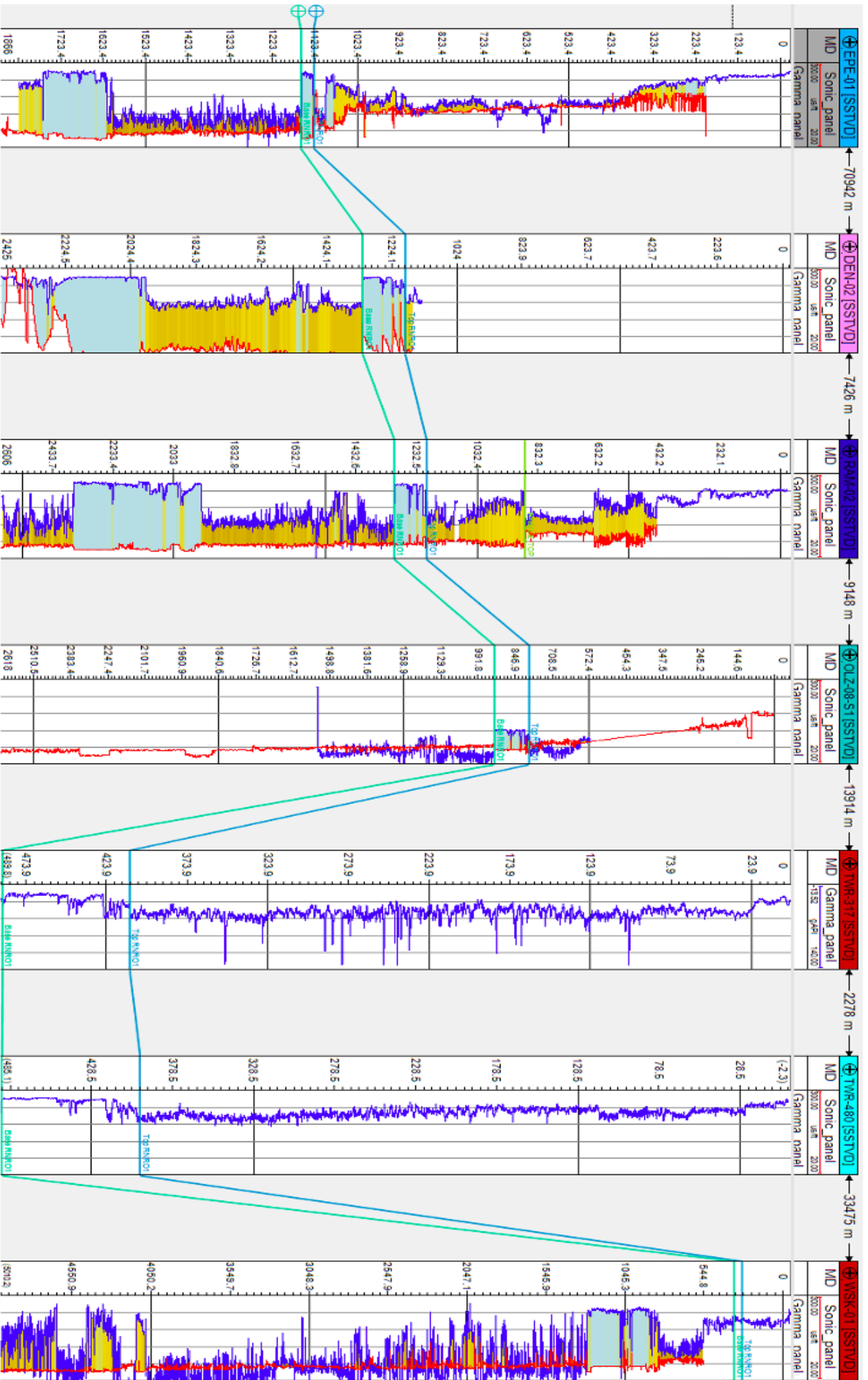


Figure 13. Well section window (next page) for different wells throughout the study area. See map for location. Blue log line = Gamma-ray log, red log line = sonic log. Blue well top line = top of the Main Röt Evaporite Member; Green well top line = base of the Main Röt Evaporite Member. Note that the Main Röt Evaporite Member has a remarkable lower gamma-ray response with different peaks, the reason for this are the different facies. Only in one well, these peaks are not visible: EPE-01 in the west of the study area which could imply different facies.



4. Discussion

Tectonic setting and events

The distribution map (Fig. 6) shows a sharp boundary in the south which is characterized by an unconformity (Fig. 7). This sharp transition is most probably fault-controlled because this boundary runs parallel with the margin of the Central Netherlands Basin (Fig. 14) (Geluk, 2005). The faults active during the Triassic were mostly N-S trending extensional faults which split up the Southern Permian Basin at the Gluckstadt and Horn Grabens (Best et al., 1983; Geluk & Röling 1999; Geluk, 2005). Besides this, also WNW-ESE faults were active e.g. the Mid Netherlands, Gronau and the North Dogger fault zones (Geluk, 2005; 2007). These faults are interpreted by Geluk (2005) as transcurrent faults and are characterized by locally preserved upper Triassic sediments in their hanging-wall block. Therefore the sharp boundary represents the division between the hanging wall and the footwall block of the mid-Netherlands fault zone whereafter the footwall block has been eroded, the reason why the Mesozoic strata are missing here (Fig. 7). For this reason, occurrences of MREM in the hanging walls of the Mid Netherlands fault zone and the Gronau fault zone indicate synsedimentary movements during evaporite deposition.

Besides this, the Gronau fault zone caused deepening of the strata in the hanging wall block, therefore a depth difference can be observed in the northeast. There is a difference in depth between the hanging wall, where a thick Main Röt Evaporite Member is preserved, and the footwall where only a small bit of the Member is preserved (Fig. 9, Fig. 14).

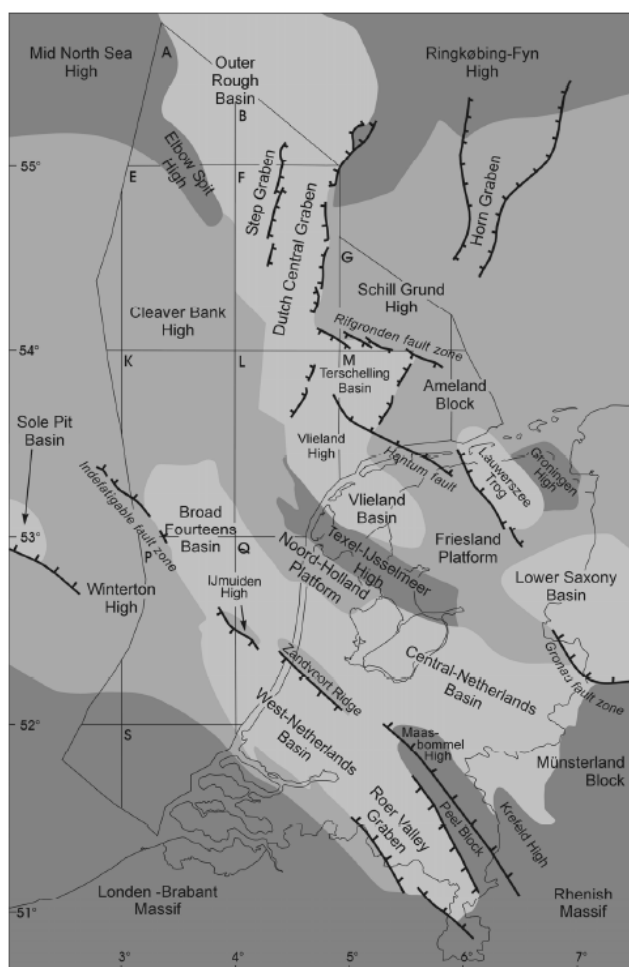


Figure 14. *Structural elements in the Netherlands during the Jurassic and Cretaceous which is a clue to the distribution of the Röt Formation. The boundary of the Central Netherlands Basin runs parallel with the boundary of the Main Röt Evaporite Member in the Triassic, which implies fault controlled. The hanging wall block of the Gronau fault zone is exactly at the location with the deepest and thickest Main Röt Evaporite Member which implies the Röt Formation is syn-sedimentary. Darker = higher; whiter = lower. In the highest areas the Triassic is removed, and the white areas represent areas of subsidence and extension during the Triassic. (After Van Adrichem Boogaert & Kouwe, 1993; Geluk, 2005).*

The thickness and depth of the Main Röt Evaporite Member is depending on the rate of subsidence and inversion of the basin. Overall, the thickness of the Main Röt Evaporite Member in the study area varies between 10 and 130 m (Fig. 9) and the depth between ≈ 150 and ≈ 1450 m (Fig. 10). The thickest Main Röt Evaporite Member lies in the northeast of the study area, where the Member is up to 130 m thick and lies relatively deep (≈ 1200 m deep). Besides the Gronau fault zone explanation, this also was the area (the Ems low) where strong subsidence occurred during the Cimmerian tectonic phase in the Triassic. Other areas where strong subsidence occurred during the Triassic generally have a thick Rot sequence, such as the Dutch Central

Graben where the MREM is up to 150 m thick and lies 3000-4000 m deep (Geluk and Röhlings, 1999; NLOG database), the Roer Valley Graben and the Central Netherlands basin (Geluk, 1996, 2005). This would suggest that in areas where most subsidence occurred during the Cimmerian tectonic phase the Main Röt Evaporite Member lies the deepest and is also relatively thick. Mckie and Kilhams (in press) describe that the Triassic strata that subsided during the Kimmerian are protected from erosion which agrees with Geluk (2005) and the results from this study because the thickest Main Röt Evaporite is present in areas that are part of subsiding regions: the Central Netherlands and the Ems Low. This would suggest that the boundary of the subsiding basin is probably where the unconformity of figure 7 lies. Whereas the footwall block has been eroded and an unconformity complied.

The thickness and distribution of the Triassic strata are determined by subsidence and inversion further limited the Triassic thickness and distribution. At the end of the Cretaceous, almost all the Triassic strata exposed have been eroded due to Alpine inversion, except for the basins that were subsided during extensional phases such as the Cimmerian as we see in the study area (Fig. 7) (e.g. Central Netherlands basin and Ems Low) but also the Dutch Central Graben is an example of this (Mckie & Kilhams, in press). The inversion caused uplift by compression of the Triassic strata, especially onshore inversion rates are high, this could also explain the difference in depth onshore and offshore (Fig. 9) (Mckie & Kilhams, in press).

The Alpine inversion at the beginning of the Late Cretaceous is not only an explanation for the erosion of the uplifted strata, but it also explains the folds we see in the area (Fig. 7, 8). Inversion also caused locally extensive fracturing of the now lithified Triassic (Mckie & Kilhams, in press). The Hardegsen phase caused swells in north-western Europe, only in the Netherlands, the swells are covered by the Röt salt causing tectonic activity in the salt during the deposition in the form of faults (Geluk, 2005). De Jager (2003) described that the presence of these faults probably is related to the Cretaceous inversion in the area. Further research has to elaborate on the faults in the Main Röt Evaporite Member.

Palaeogeography and facies distribution

The facies that have been described for well TWR-480 (Table 3) fit well in the saline mudflat sabkha facies and shallow water evaporite facies as described by Kendall (2010) but could also fit well in the Playa-Lake model proposed by Eugster & Hardie (1975). Sabkha, in other words, a saline mudflat, is supplied by seawater flooding, by continental groundwaters or they occur close to saline lakes, salt pans or the sea (Kendall, 2010). In contrast, saline playa-lake environments are restricted continental and fed by runoff and/or groundwater discharge (Renaut and Gierlowski-Kordesch, 2010). Research by several authors has shown that the source of the salt of the Röt Formation was marine water (Holser and Wilgus 1981; Czapowski et al. 1992; Kovalevych et al. 2002; Paul 2006; Kovalyvetch, 2009). Based on this, a saline playa-lake environment is less obvious while a saline mudflat sabkha facies supplied by seawater flooding is straightforward.

Saline mud flat sabkha facies are facies that are described as ‘a chaotic mix of evaporite crystals within an unlaminated matrix’ – Kendall (2010) which we see in Facies E, F and H (Fig. 11.5, 11.6, 11.8). The laminated dolomites (Facies B, Fig. 11.2) can be interpreted as hypersaline lagoon facies that fit within a sabkha cycle (Kendall, 2010). Facies C (Fig. 11.3) can be described as efflorescent halite alternated with chevron halite as Lowenstein (2003) described where the environment is a subaerial mudflat as the Atacama basin today (Lowenstein, 2003). The chickenwire structures from facies D (Fig. 11.4) can be interpreted as typical supratidal sediments from a sabkha (Kendall, 2010). In different facies, laminae are observed (Facies B, H and J, Fig. 11.2, 11.8, 11.10) which occur within evaporites deposited in an episodically flooded environment (Kendall, 2010). If this is the case it would fit in the sabkha environment that gets flooded from time to time, leaving a layer of water where clear crystalline halite can form. The microcrystalline facies, facies A, D, G and I (Fig. 11.1, 11.4, 11.7, 11.9) are probably shallow-water evaporites which form in brines less than 5 m deep and are typically surrounded by evaporite-flats (Kendall, 2010).

The salt pan model as proposed by Lowenstein and Hardie (1985) can be an explanation for the facies and interbedded clay layers. The features of the bedded salt of the Main Röt Evaporite Member that has been found in TWR-480 fit very well in the salt pan model described by Lowenstein and Hardie (1985). The salt pan model describes a model of how layered halite develops in a dry shallow depression that gets overflowed by unsaturated water in stages. Water dissolves the old salt crust for a part whereafter the

water is saturated again and crystallization starts at the surface of the pond while at the bottom the crystals collect and grow together (Lowenstein & Hardie, 1985). Within the salt pan model, the clay layers are formed by the dissolution of halite containing dispersed clay during an incursion of fresh seawater (Lowenstein & Hardie 1985).

Salt pans grade insensibly into sabkha environments where evaporites accumulate as detrital sediments (Kendall, 2010). This could explain the alternation between the salt pan and the sabkha facies.

The salt pan facies model surrounded by sabkha facies agrees with earlier facies interpretations of the whole Röt Formation. The depositional setting of the Röt Formation has earlier been interpreted as a shallow, brackish, evaporitic basin with a restricted connection between the Tethys Ocean and the Western Southern Permian Basin surrounded by sabkhas where terrestrial fauna lived on the mudflats which received an influx of clastics from southern sources (Warrington, 1974; Riddler, 1981; Schröder, 1982; Cameron et al., 1992; Geluk, 1996; Diedrich & Cajus, 2001; Geluk, 2005). Work by Cajus & Diedrich gives a more detailed facies model in smaller units of about one and a half to one million years in length (Cajus & Diedrich, 2009). This shows that from time to time the study area was covered in a salt pan surrounded by sabkha, which had restricted marine access (Fig. 15).

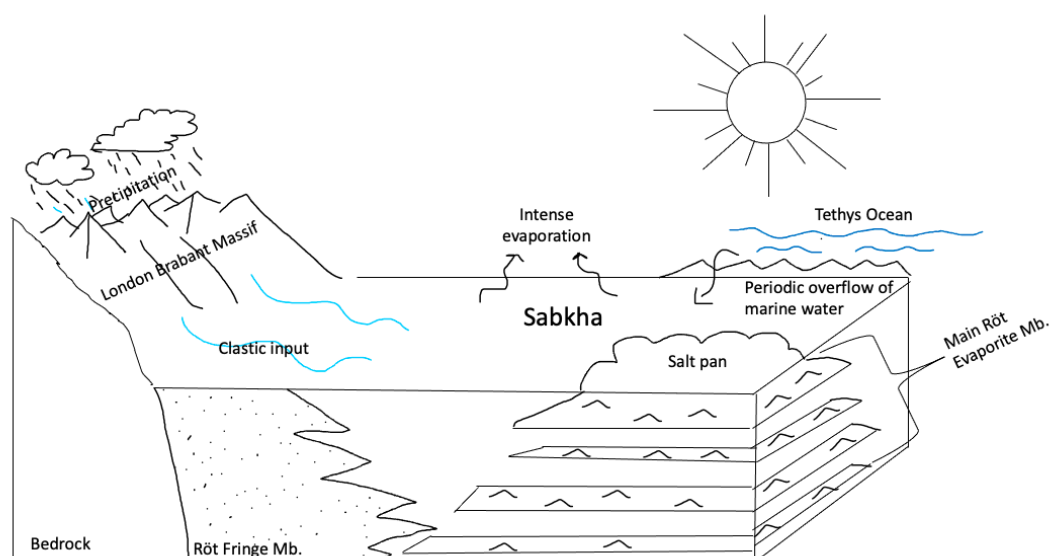


Figure 15. *Depositional setting for the Main Röt Evaporite Member in the Netherlands. Sabkha environment with salt pans with restricted marine influence from the Tethys Ocean in the east. The sabkha is periodically overflowed by marine water which leaves saturated salt pans where microcrystalline halite can form. Coarsely crystalline halite develops on the sabkha and with gravitational movements in the salt pan. Clastic input is coming from the south, due to precipitation, here the Röt Fringe Member develops.*

In the Palaeographic setting of the Röt Formation, the clastic input came from the south, by fluvial systems from the London-Brabant, Rhenish, Bohemian and Vindelician massifs, this possibly reflects an increase in precipitation (Bachmann et al., 2010) and could be an explanation for the clay. In the West Netherlands Basin and the Off Holland Low, the clastic part onlaps onto the Solling Formation and the evaporitic part of the Röt Formation is missing while in the Roer Valley Graben both the clastic and evaporitic part of the Röt Formation is present (Geluk, 1996). The Röt has in the Roer Valley Graben and in the West Netherlands Basin the Röt Fringe Sandstone Member, which represents the last clastic input in the Triassic (Geluk, 1996). Only areas with a reduced Main Bunsandstein succession,

Netherlands Swell and Celaverbankn high, show deposition of the Main Röt Evaporite Member. (Geluk, 2005). In contrast, in areas with major subsidence during the Main Buntsandstein Group, (West Netherlands Basin and the Off Holland low) the Röt Formation is less than 50 m thick (Geluk, 1996).

Crystalline vs mechanical facies

Different facies have been described (Table 3), a remarkable aspect is the structure of the salt, there are microcrystalline and coarsely crystalline halite facies. Evaporites normally exhibit a microcrystalline fabric in which crystals interlock to form a sealing fabric with virtually no porosity or permeability (Hunsche and Hampel, 1999). Under certain environmental circumstances, however, such as debris flows, evaporites may be eroded and redeposited as detrital particles (Kendall, 2010).

Overall, the different evaporitic facies in well TWR-480 are partly reworked except for facies A, D, G, and I where the clearest homogenous microcrystalline halite is present (not considering the small clay particles). Facies B, C, E, F and H have some mechanically deformed salt crystals and have therefore a higher permeability than the microcrystalline halite facies.

In some facies, it looks like there are broken pieces of evaporite which have been redeposited and therefore have a mechanical fabric (Facies E and F) (Fig. 11.5, 11.6). However, the process behind the reworking of the salt crystals is hard to define. This process has been studied by several authors at different salt formations with similar characteristics, whether it has been

syn-sedimentary reworking or deformation-related reworking (Wardlaw and Schwerdtner, 1966; Hardie et al., 1983; Schleder and Urai, 2005). This agrees with the observation of Schleder and Urai (2005) who studied the Main Röt Evaporite Member of well TWR-382, which is only tens of kilometres away from the studied well. They found the same features as this study: 'large blocky halite grains marked by anhydrite partings, horizontal truncation surfaces, small grains intercalated in the salt bodies and polyhalite' (Schleder & Urai, 2005).

Schleder and Urai (2005) describe that the water in the salt pan must have been so shallow that there were fluctuations in NaCl saturation and therefore in the growth rate of the crystals. They interpreted that the origin of the large blocky crystals lies in the bottom of the salt pan since the salt crystals collect there and grow together. Furthermore, in their research, they found that the halite crystals can develop enough stress so that they can interfere with other materials like clay and anhydrite. This could be an explanation for the particular facies of facies H (Fig. 11.8).

Although the salt pan model, surrounded by sabkhas does fit well for the Main Röt Evaporite Member, the broken pieces of evaporite in the clay (facies E and F) (Fig. 11.5, 11.6) are not fully explained by this. Another option for the reworked crystals and halite patches could be fault movement, as described in a study by Peryt and Kovalevich (1997).

Peryt & Kovalevitch (1997) describe halite breccias similar to the ones found in TWR-480 as gravity-induced movements, induced by tectonic

movements. A possible explanation for the facies could be that the Gronau fault zone caused syn-sedimentary movement and the facies of E and F (Fig. 11.5, 11.6) could develop by reworking of the halite, however, further study of this process is required.

Stratigraphic correlation

The well section window (Fig. 13) showed that well TWR-480 is representative for the rest of the study area. This is being strengthened by a study that is done on well TWR-382, which is ≈ 2.5 km from TWR-480 (Kovalevych 2002; Schlöder and Urai, 2005). Both the TWR-480 and TWR-382 have 4 salt layers, salt A-D with between them mainly claystones. There is some differentiation in thickness but overall the wells show very similar lithology and therefore probably facies. However, these wells are very close and can both be affected by the same fault zone. Towards the West of the Netherlands, where the Main Röt Evaporite Member is also deposited, it could be interesting to study the facies. It is deposited in the same environment as the well that is studied for this study, there will probably not be differences in the environment or clastic input, however, the mechanically reworked halite crystals could be absent there since major faults are missing in that area.

Assessment of the storage/disposal potential

In a disposal concept in Germany where disposal in the underground is considered, they used 100 m as a minimum thickness for the host rock to assure safe disposal (Lommerzheim et al., 2019). Another study by (Minkley,

2009) states that 100 m for the salt barrier thickness for flat bedded deposits like the Main Röt Evaporite Member is adequate for safe disposal (Minkley, 2009). And for storage concepts, the depth should be between 400 to 500 m and up to 2000 m (Cyran 2020).

Besides this, the formation should be deep enough so surface processes will not have influence and people cannot interfere with it (Verhoef, 2017). Therefore the depth should be several hundreds of m. For this assessment there is assumed that 250 m is sufficient depth, further study will elaborate on this.

Next to the thickness and depth of the unit, the permeability is of importance to assess its storage/disposal potential. For this study, the crystalline halite vs. the mechanically reworked halite tells us something about the permeability, although this is not exact. Homogenous microcrystalline halite is preferable, it makes the quality of the natural barrier higher. Therefore the microcrystalline facies (facies A, D, G and I) are preferred. However, these microcrystalline facies are alternated with reworked coarsely crystalline halite facies which are less preferred due to overall higher permeability. This can cause problems and further studies have to elaborate on this. For example, at the disposal concept of the Waste Isolation Power Plant (WIPP) in the USA, research has shown that interfering with clay layers can cause issues in the future (Erumhansl et al., 1990). Over time, the diagenesis of clay layers within halite may affect components used in backfilling or sealing the repository and cannot be

completely dismissed until more data is available on this matter (Erumhansl et al., 1990).

Besides this, faults play a role in the porosity and therefore permeability of the future host rock. Inversion in the Cretaceous was accompanied by faults (de Jager, 2003). Therefore, it can be suggested that the area that has been inverted the most is the area with most of the faults and is, therefore, less preferable as a host rock.

Only a small part of the Main Röt Evaporite Member satisfies the requirements that are established above. Therefore a thickness of 75 m is also suggested for a storage/disposal concept but is not preferred. With these requirements still, only a small part of the research area is potentially suitable for storage/disposal. In the north of the study area, the salt is thick enough and it lies deep enough. Furthermore, at three spots in the middle of the research area, the requirements are feasible as well. However, the spots where the requirements for the assessment are met are relatively small (≈ 2 km²). A map with an overview has been made to assess the storage and disposal potential of the Main Röt Evaporite Member of the Röt Formation (Fig. 16).

Limitations

An uncertainty of this study is the interpretation of the seismic data. The continuation and amplitude of the seismic reflections were not always ideal for interpretation, another person's interpretation is likely to be at least a little different from the one presented in this thesis. Another uncertainty is

the number of wells and especially the distribution of these. The wells that were used in this study are not evenly spread over the study area, most of the wells are concentrated in the central part of the study area, around Enschede (Fig. 3). For this study, only 12 key wells are used, while there are more wells in the area that could have valuable information for the Röt Formation.

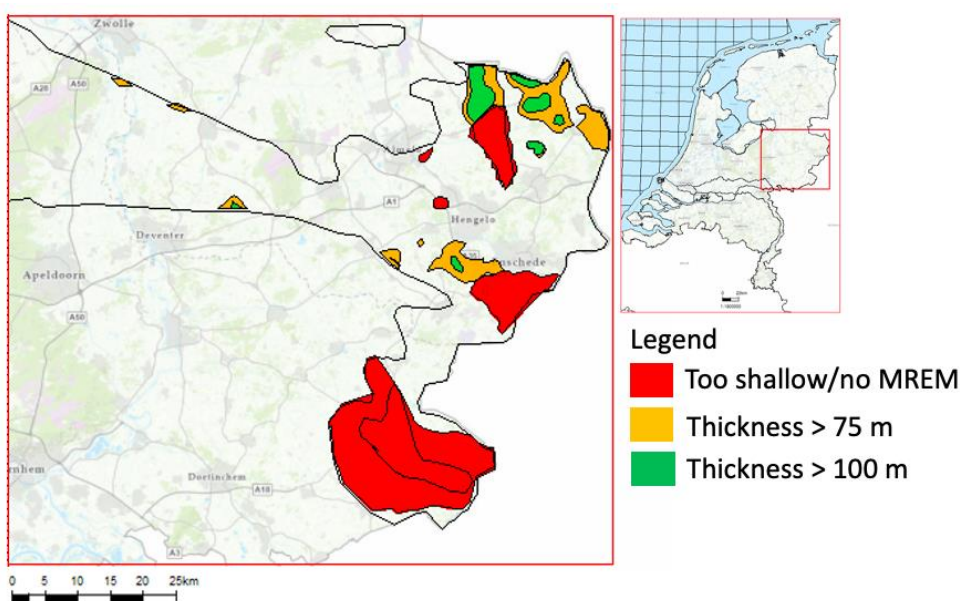


Figure 17. Assessment for the storage/disposal potential of the Main Röt Evaporite Member in the east of the Netherlands based on the distribution, depth and thickness maps. The red areas show the areas with insufficient thickness, the orange and green areas show where the thickness is possibly sufficient, the area without a colour does not have sufficient thickness and is therefore not suitable as storage/disposal. The area that is potentially suitable for storage/disposal is around Enschede, however; the thickness here ranges between 75 m and 100 m which is in most concepts not enough. In the north of the study area it could be potentially suitable as storage/waste since the thickness is over the required 100 m, this is an area of approximately 2 km².

Recommendations

This study shows that the Main Röt Evaporite Member in this study area is only a small part suitable for storage/disposal. However, the MREM is more widespread in the Netherlands, it would therefore be interesting to characterize the storage/disposal potential in the rest of the Netherlands.

Especially the west of the Netherlands, the province of Noord Holland, could have potential. If the Gronau fault zone was partly the reason for this sequence of facies, it could be very well possible that the halite is more microcrystalline, and thus preferred as a storage/disposal, towards the west of the study area.

Only one well has been studied in detail (TWR-480), I would recommend studying more wells and making more facies interpretations to check if the facies agree with the one presented in this study. Due to the different Gamma-ray responses, it is interesting to check if the same facies can be found in the EPE-01 well and the west of the study area. In the area where the requirements for a potential storage/disposal concept have been met, a study towards the exact porosity would be recommended, regarding the amount (%) of interfering facies and faults.

5. Conclusions

- The thickness of the Main Röt Evaporite Member in the study area ranges between 10 and 130 m the thickest parts are around Enschede in the centre of the study area and Tubbergen in the north.
- The depth of the Main Röt Evaporite Member in the study area ranges between 300 and 1500 m. The Member is the deepest in the north of the study area, around Tubbergen, and the most shallow in the south, around Winterswijk.
- The distribution of the Main Röt Evaporite Member is controlled by the shape of the Triassic extensional basin and the inversion rate in the area during the Late Cretaceous
- The depositional environment of the Main Röt Evaporite Member is a marginal-marine sabkha that over time interacts with marine waters leaving salt pans.
- The Main Röt Evaporite Member is in a small part of the study area, around Enschede, potentially suitable for storage and disposal.
- Based on other disposal concepts the Main Röt Evaporite Member in the study area is not reliable for disposal.

References

- Best, G., Kockel, F. & Schöneich, H. (1983) Geological history of the southern Horn Graben. In: Kaasschieter, J.P.H. & Reijers, T.J.A. (eds): Petroleum geology of the southeastern North Sea and the adjacent onshore areas. *Geologie en Mijnbouw* 62: 25–33.
- Bachmann, G.H., Beutler, H., Hagdorn, N., Hauschke, N. (1999) Stratigraphie der Germanischen Trias. N. Hauschke, V. Wilde (Eds.), *Trias-Eine ganz andere Welt. Europa am Beginn des Erdmittelalter*, Pfeil, München (1999), pp. 83-106
- Bachmann, G.H., Geluk, M.C., Warrington, G., Becker-Roman, A., Beutler, G., Hagdorn, H., Hounslow, M.W., Nitsch, E., Röhling, H.-G., Simon, T. & Szulc, A., (2010) Triassic. In: Doornenbal, J.C. and Stevenson, A.G. (editors): *Petroleum Geological Atlas of the Southern Permian Basin Area*. EAGE Publications b.v. (Houten): 149-173.
- Baldschuhn, R., Binot, F., Fleig, S. & Kockel, F. (2001) *Geotektonischer Atlas von Nordwestdeutschland und dem deutschen Nordsee-Sektor*. Geol. Jb. A153, 95 pp. (3 CDRoms).
- Bertelsen, F. (1980) Lithostratigraphy and depositional history of the Danish Triassic. Geological Survey of Denmark, Series B 4: 59 pp.
- Cameron, T.D.J., Crosby, A., Balson, P.S., Jeffery, D.H., Lott, G.K., Bulat, J. & Harrison, D.H. (1992) *United Kingdom Offshore Regional Reports: The geology of the southern North Sea*. HMSO for British Geological Survey: 152 pp.
- Czapowski, G., Peryt, T.M., Raup, O.B. (1992) Carbonate-anhydrite-halite cycles in the Roet (Lower Triassic) of western Poland: *Bulletin of the Polish Academy of Sciences, Earth Sciences*, v. 40, p. 161-164.
- Cohen, K.M., Finney, S.C., Gibbard, P.L. & Fan, J.-X. (2013) (updated). The ICS International Chronostratigraphic Chart. *Episodes* 36: 199 – 204. <https://doi.org/10.18814/epiiugs/2013/v36i3/002>.
- Cyran, K. (2020) Insight into a shape of salt storage caverns. *Arch. Min. Sci.*, 65, 363–398.
- Dadlez, R., Marek, S. & Pokorski, J. (eds) (1998) *Atlas Paleogeograficzny Epikontynentalnego Permu I Mesozoiku w Polsce (Paleogeographical Atlas*

of the Epicontinental Permian and Mesozoic in Poland (1: 2,500,000).
Panstwowy Instytut Geologiczny (Warszawa).

Diedrich, C.G. (2009) Palaeogeographic evolution of the marine Middle Triassic marine Germanic Basin changes – With emphasis on the carbonate tidal flat and shallow marine habitats of reptiles in Central Pangaea, *Global and Planetary Change*, Volume 65, Issues 1–2, Pages 27–55, <https://doi.org/10.1016/j.gloplacha.2008.11.002>.

Erumhansl, J.L., Kimball, K.M., Stein, C. L. (1990) A Review of WIPP Repository Clays and their Relationship to Clays of Adjacent Strata. Geochemistry Division 6233, Sandia National Laboratories, Albuquerque, NM 87185

Geluk, M.C. (1999) Palaeogeographic and structural development of the Triassic in the Netherlands –new insights. In: Bachmann, G.H. & I. Lerche (eds) *The Epicontinental Triassic*, Halle, *Zentralblatt für Geologie und Paläontologie* 1998: 727–745.

Geluk, M.C. (2005) Stratigraphy and tectonics of Permo-Triassic basins in the Netherlands and surrounding areas. PhD thesis, Utrecht University: 171 pp.

Geluk, M.C. (2007) Triassic. *Geology of the Netherlands*, pp. 85-106. Edited by Th.E. Wong, D.A.J. Batjes & J. de Jager Royal Netherlands Academy of Arts and Sciences.

Geluk, M.C., Paar, W.W., Fokker, P.A. (2007) Salt. *Geology of the Netherlands*, pp. 283-294. Edited by Th.E. Wong, D.A.J. Batjes & J. de Jager Royal Netherlands Academy of Arts and Sciences.

Geluk, M.C., Röhling, H-G. (1997) High-resolution sequence stratigraphy of the Lower Triassic “Buntsandstein” in The Netherlands and northwestern Germany. *Geologie en Mijnbouw* 76:227–246

Geluk, M.C. & Röhling, H.-G. (1999) High-resolution sequence stratigraphy of the Lower Triassic Buntsandstein: a new tool for basin analysis. In: Bachmann, G.H. & I. Lerche (eds): *The Epicontinental Triassic*, *Zentralblatt für Geologie und Pal.ontology* 1998: 545–570.

Geowulff laboratories. Lithological study of Well TWR-480 for Akzo Nobel Base Chemical bv. Prepared by Geowulff laboratories, The Netherlands (found in the well information on NLOG).

Goldsmith, P.J., Hudson, G. & Van Veen, P. (2003) Triassic. In: Evans, D., Graham, C., Armour, A. & Bathurst, P. (editors and co-ordinators): *The Millennium Atlas: petroleum geology of the central and northern North Sea*, Geological Society (London): 105–127

Hansen, F., Kuhlman, K., Sobolik, S. (2016) Considerations of the differences between bedded and domal salt pertaining to disposal of heat-generating nuclear waste. Sandia National Lab.

Hardie, L.A., Lowenstein, T.K., Spencer, R.J. (1983) The problem of distinguishing between primary and secondary features in evaporites. In: Schreiber, B.C., Harner, H.L. (eds) 6th symposium on salt. Salt Institute, Alexandria, pp 11–39

Harsveldt HM (1980) Salt resources in The Netherlands as surveyed by AKZO. In: Coogan AH, Hauber L (eds) 5th symposium on salt. Hamburg, Germany, pp 65–8

Holser, W.T., Wilgus, C.R. (1981) Bromide profiles of the Rot salt, Triassic of northern Europe, as evidence of its marine origin: *Neues Jahrbuch für Mineralogie Monatshefte*, no. 6, p. 267-276.

Hunsche, U., Hampel, A. (1999) Rock salt — the mechanical properties of the host rock material for a radioactive waste repository, *Engineering Geology*, Volume 52, Issues 3–4, Pages 271-291, [https://doi.org/10.1016/S0013-7952\(99\)00011-3](https://doi.org/10.1016/S0013-7952(99)00011-3).

de Jager J. (2003) Inverted basins in The Netherlands, similarities and differences. *Geologie en Mijnbouw* 82(4):355–366

Kendall, A.C. & Harwood, G.M. (1996) Chapter 8 Marine evaporites: rid shorelines and basins. In Harold G. Reading (Ed), *Sedimentary Environments: Processes, Facies and Stratigraphy* (pp. 281 – 324) John Wiley & Sons

Kendall, A.C. (2010) Chapter 20 Marine Evaporites. In Noel P. James and Robert W. Dalrymple (Eds), *Facies models 4* (pp. 505-540) Geological Association of Canada.

Kilhams, B., Stevanovic, S. & Nicolai, C. (2018) The ‘Buntsandstein’ gas play of the Horn Graben (German and Danish offshore): dry well analysis and remaining hydrocarbon potential. In: Kilhams, B., Kukla, P. A., Mazur, S., Mckie, T., Mijnlieff, H. F. & van Ojik, K. (eds): *Mesozoic Resource*

Potential in the Southern Permian Basin. Geological Society, London, Special Publications 469: 149 – 168. <https://doi.org/10.1144/SP469.19>.

Kovalevych, V., Peryt, T.M., Beer, W., Geluk, M., Halas, S. (2002) Geochemistry of Early Triassic seawater as indicated by study of the Rot halite in The Netherlands, Germany, and Poland. *Chem Geol* 182(2–4):549–563

Kovalevych, V., Paul, J., Peryt, T.M. (2009) Fluid inclusions in halite from the Röt (Lower Triassic) salt deposit in central Germany: Evidence for seawater chemistry and conditions of salt deposition and recrystallization. *Carbonates and Evaporites*. 24. 10.1007/BF03228056.

Kozur, H. (1974) Probleme der Triasgliederung und Parallelisierung der germanischen und tethyalen Trias Freiberger Forschungshefte. C, 298, pp. 139-197

Lommerzheim, A., Jobmann, M., Meleshyn, A., Mrugalla, S., Rübel, A., Stark, L. (2019) Safety concept, FEP catalogue and scenario development as fundamentals of a long-term safety demonstration for high-level waste repositories in German clay formations", Multiple Roles of Clays in Radioactive Waste Confinement, S. Norris, E.A.C. Neeft, M. Van Geet

Lowenstein TK, Hardie LA (1985) Criteria for the recognition of salt-pan evaporites. *Sedimentology* 32:627–644

Lowenstein, T. K., Hein, M.C., Bobst, A. L., Jordan, T. E., Ku, T-L. and Luo, S. (2003) An assessment of stratigraphic completeness in climate-sensitive, closed-basin lake sediments: Salar de Atacama, Chile: *Journal of Sedimentary Research*, v. 73, p. 91-104.

McKie, T. & Kilhams, B. (in press) Triassic. *Geology of the Netherlands*.

Neeft, E., Bartol, J., Vuorio, M. (in press) Geological Disposal of Radioactive Waste. *Geology of the Netherlands*.

NITG (1998) Geological Atlas of the subsurface of the Netherlands, Explanation to map sheet X Almelo-Winterswijk. Netherlands Institute for Applied Geoscience TNO, Haarlem, 134 pp.

Paul, J. (2006) Facies analysis and sequence stratigraphy of an evaporitic-fluviatile unit : The Rot (Lower Triassic, Germany): *Neues Jahrbuch für Geologie und Paläontologie Abhandlungen*, v. 242, p. 103-132.

Peryt, T.M., Kovalevych, V.M. (1997) Association of redeposited salt breccias and potash evaporites in the lower Miocene of Stebnyk (Carpathian Foredeep, West Ukraine). *Journal of Sedimentary Research*, 67 (5): 913–922. doi: <https://doi.org/10.1306/D4268676-2B26-11D7-8648000102C1865D>

Popp, T., Kern, H., & Schulze, O. (2001) Evolution of dilatancy and permeability in rock salt during hydrostatic compaction and triaxial deformation. *J. Geophys. Res. Solid Earth*(106), 4061-4078.
doi:<https://doi.org/https://doi.org/10.1029/2000JB900381>

Remmelts, G., (1996) Salt tectonics in the southern North Sea, the Netherlands. In: Rondeel, H.E., Batjes, D.A.J. & Nieuwenhuijs, W.H. (eds): *Geology of Gas and Oil under the Netherlands*. Kluwer (Dordrecht): 143–158

Renaut, R.W., Gierlowski-Kordesch, E.H. (2010) Chapter 21 Lakes. In Noel P. James and Robert W. Dalrymple (Eds), *Facies models 4* (pp. 541-576) Geological Association of Canada.

Schleder, Z., & Urai, J.L. (2005). Microstructural evolution of deformation-modified primary halite from the Middle Triassic Röt Formation at Hengelo, The Netherlands. *International Journal of Earth Sciences*, 94, 941-955.

Spiers, C., Peach, C., Brzesowsky, R., Schutjens, P., Liezenberg, J., & Zwart, H. (1988). Long-term rheological and transport properties of dry and wet salt rocks. Commission of the European Communities.

Southworth, C.J. (1987) Lithostratigraphy and depositional history of the middle triassic dolomitic formation of the southern north sea and adjoining areas, University of Oxford, PhD thesis

TNO-GDN (2022). Solling Formation. In: *Stratigraphic Nomenclature of the Netherlands*, TNO – Geological Survey of the Netherlands. Accessed on 27-03-2022 from <http://www.dinoloket.nl/en/stratigraphic-nomenclature/solling-formation>.

Trammer, J. (1972) *Beyrichites (Beyrichites) sp.* from the Lower Muschelkalk of the Holy Cross Mts *Acta Geologica Polonica*, 22, pp. 25-28

Urai, J., Schlöder, Z., Spiers, C., & Kukla, P. (2008). Chapter 5.2 Flow and transport properties of salt rocks. In *Dynamics of complex intracontinental basins: The central European basin system* (pp. 277-290).

van Adrichem-Boogaert, H.A. and Kouwe, W.F.P. (1993-1997),
Stratigraphic nomenclature of the Netherlands; revision and update by RGD
and NOGEPa, Mededelingen Rijks Geologische Dienst, vol. 50, Haarlem.

van Wees, J.-D., Stephenson, R.A., Ziegler, P.A., Bayer, U., McCann, T.,
Dadlez, R., Gaupp, R., Narkiewicz, M., Bitzer, F. & Scheck, M. (2000) On
the origin of the Southern Permian Basin, Central Europe. *Marine and
Petroleum Geology* 17: 43 – 59. [https://doi.org/10.1016/S0264-
8172\(99\)00052-5](https://doi.org/10.1016/S0264-8172(99)00052-5).

Wardlaw NC, Schwerdtner WM (1966) Halite-Anhydrite seasonal layers in
the Middle Devonian Prairie Evaporite Formation, Saskatchewan, Canada.
Geol Soc Am Bull 77:331–342

Warren J.K., (2006) *Evaporites: sediments, resources and hydrocarbons*.
Springer Springer-Verlag Berlin Heidelberg, 1042 pp.

Wolburg, J. (1969) Die epirogenetischen Phasen der Muschelkalk- und
Keuper-Entwicklung Nordwest-Deutschlands, mit einem Rückblick auf den
Buntsandstein. *Geotektonische Forschungen* 14: 7–74.

Ziegler, P.A. (1990) *Geological Atlas of Western and Central Europe*.
Second edition, Geological Society Publishing House (Bath): 239 pp.

Appendix

Seismic surveys used in this study

	Name	year	company	type	n of lines
1	L2NAM1970	1970	NAM	2D	32 lines
	706001_____mig160001				
	706005_____mig160001				
	706006_____mig160001				
	706008_____mig160001				
	706009_____mig160001				
	706011_____mig160001				
	706012_____mig160001				
	706018_____mig160001				
	706019_____mig160001				
	706022_____mig160001				
	706024_____mig160001				
	706025_____mig160001				
	706026_____mig160001				
	706027_____mig160001				
	706028_____mig160001				
	706029_____mig160001				
	706031_____mig160001				
	706032_____mig160001				
	706033_____mig160001				
	706034_____mig160001				
	706035_____mig160001				
	706036_____mig160001				
	706039_____mig160001				
	706040_____mig160001				
	706041_____mig160001				
	706042_____mig160001				
	706044_____mig160001				
	706045_____mig160001				
	706046_____mig160001				
	706047_____mig160001				
	706049_____mig160001				
	706051_____mig160001				
2	L2NAM1971	1971	NAM	2D	39 lines
	716004_____mig160001				
	716005_____mig160001				
	716007_____mig160001				

	716008	mig160001				
	716009	mig160001				
	716010	mig160001				
	716011	mig160001				
	716013	mig160001				
	716014	mig160001				
	716017	mig160001				
	716018	mig160001				
	716019	mig160001				
	716020	mig160001				
	716021	mig160001				
	716023	mig160001				
	716025	mig160001				
	716026	mig160001				
	716028	mig160001				
	716029	mig160001				
	716030	mig160001				
	716031	mig160001				
	716032	mig160001				
	716033	mig160001				
	716034	mig160001				
	716035	mig160001				
	716036	mig160001				
	716038	mig160001				
	716039	mig160001				
	716040	mig160001				
	716041	mig160001				
	716042	mig160001				
	716044	mig160001				
	716046	mig160001				
	716051	mig160001				
	716053	mig160001				
	716055	mig160001				
	716056	mig160001				
	716064	mig160001				
	716066	mig160001				
3	L2NAM1972		1972	NAM	2D	23 lines
	726006	mig160001				
	726008	mig160001				
	726010	mig160001				
	726020	mig160001				
	726022	mig160001				
	726024	mig160001				

	726026	mig160001				
	726027	mig160001				
	726029	mig160001				
	726030	mig160001				
	726031	mig160001				
	726032	mig160001				
	726033	mig160001				
	726033X	mig160001				
	726034	mig160001				
	726035	mig080001				
	726036A	mig160001				
	726037	mig160001				
	726038	mig160001				
	726039	mig160001				
	726047	mig160001				
	726049	mig160001				
	726051	mig160001				
4	L2NAM1973		1973	NAM	2D	8 lines
	732201	mig160001				
	732202	mig160001				
	732204	mig160001				
	732205	mig160001				
	732206	mig160001				
	732208	mig160001				
	732209	mig160001				
	732210	mig160001				
5	L2NAM1975		1975	NAM	2D	18 lines
	751051	mig160001				
	751052	mig160001				
	751053	mig160001				
	751054	mig160001				
	751055	mig160001				
	751056	mig160001				
	751057	mig160001				
	751058	mig160001				
	751059	mig160001				
	751060	mig160001				
	751062	mig160001				
	751064	mig160001				
	751065	mig160001				
	751066	mig160001				
	751067	mig160001				
	751068	mig160001				

	751069_____mig160001				
	751070_____mig160001				
6	L2NAM1982	1982	NAM	2D	28 lines
	823101_____mig160001				
	823102_____mig160001				
	823103_____mig160001				
	823104_____mig160001				
	823105_____mig160001				
	823107_____mig160001				
	823108_____mig160001				
	823109_____mig160001				
	823110_____mig160001				
	823111_____mig160001				
	823112_____mig160001				
	823113_____mig160001				
	823114_____mig160001				
	823115_____mig160001				
	823116_____mig160001				
	823117_____mig160001				
	823118_____mig160001				
	823119_____mig160001				
	823120_____mig160001				
	823121_____mig160001				
	823122_____mig160001				
	823123_____mig160001				
	823124_____mig160001				
	823125_____mig160001				
	823126_____mig160001				
	823127_____mig160001				
	823129_____mig160001				
	823133_____mig160001				
7	L2PET1983D	1983	Delft Geophysical	2D	2lines
	1463519_12417				
	1463516_12417				
8	L3NAM1993A	1993		3D	